7-Hydroxyquinoline-8-carbaldehydes. 1. Ground- and Excited-State Long-Range Prototropic Tautomerization

ARTICLE *in* THE JOURNAL OF PHYSICAL CHEMISTRY A · SEPTEMBER 2013

Impact Factor: 2.69 · DOI: 10.1021/jp403621p · Source: PubMed

THE JOURNAL OF PHYSICAL CHEMISTRY A

Article

pubs.acs.org/JPCA

7-Hydroxyquinoline-8-carbaldehydes. 1. Ground- and Excited-State Long-Range Prototropic Tautomerization

Volha Vetokhina,[†] Jacek Nowacki,[‡] Mariusz Pietrzak,[†] Michał F. Rode,[§] Andrzej L. Sobolewski,[§] Jacek Waluk,[†,∥] and Jerzy Herbich*[,†,∥]

[†]Institute of Physical Chemistry, Polish Academy of Sciences, Kasprzaka 44/52, 01-224 Warsaw, Poland

[‡]Department of Chemistry, Warsaw University, Pasteura 1, 03-093 Warsaw, Poland

[§]Institute of Physics, Polish Academy of Sciences, al. Lotników 32/46, 02-668 Warsaw, Poland

[∥]Faculty of Mathematics and Science, Cardinal Stefan Wyszyński University, Dewajtis 5, 01-815 Warsaw, Poland

Supporting Information

ABSTRACT: Ground- and excited-state long-range prototropic tautomerization were studied for a series of 7-hydroxyquinoline-8-carbaldehydes (**7-HQCs**) by ^{1}H and ^{13}C NMR spectroscopy, photostationary and time-resolved UV−vis spectroscopic methods, and quantum chemical computations. These molecules represent trifunctional proton-donating/accepting systems that have been proposed to serve as models of a reversible optically driven molecular switch composed of two moieties: a molecular "frame" (7-hydroquinolines, **7-HQs**) and a proton "crane" (carbaldehyde group). The NMR and electronic absorption spectra indicate a solvent-dependent equilibrium between two tautomeric forms, **OH** (7-quinolinol)) and **NH** (7(1*H*)-quinolinone), already in the ground state of all the compounds under study (7-hydroxy-2-methoxy-4-methylquinoline-8-carbaldehyde, **HMMQC**, shows only a trace of the **NH** form in highly polar and/or protic media). Electronic absorption and fluorescence of **7-HQCs** are rationalized in terms of the ground- and excited-state hydrogen atom transfer (HAT). This process was identified by comparing the UV−vis spectroscopic properties of **7-HQCs** with those of **7-HQs**, synthetic precursors of the former, as well as with the characteristics of corresponding protonated cations and deprotonated anions (part 2). The experimental results are corroborated by the density functional theory (DFT) and ab initio computations, which shed some light on the differences in photophysics between variously substituted **7-HQCs**.

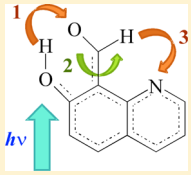

1. INTRODUCTION

Ground- and excited-state proton-transfer (ESPT) reactions are among the most important processes in chemistry and biology.[1−10] Particular attention is paid to heteroaromatic bifunctional molecules that can simultaneously act as hydrogen bonding donors and acceptors and may reveal simultaneous enhancement of acidity and basicity upon electronic excitation, which provides a driving force for ESPT processes. Photoinduced tautomerization in molecules with strong intramolecular hydrogen bonds, which provide the suitable geometry for the rapid, barrierless or nearly barrierless, process can be detected even at very low temperatures under isolated solvent-free supersonic jet conditions. For instance, excited-state intramolecular proton transfer (ESIPT) has been observed in molecular beams for 2,5-bis(2′-benzoxazolyl)-hydroquinone,[11] methyl salicylate,[12−16] salicylic acid,[17,18] *o*-hydroxyacetophenone,[19,20] their related systems,[16,19] and 2-(2′-pyridyl)pyrrole[21] (PP, also in a gas phase[22]). If there is no intramolecular hydrogen bond (HB) present, the phototautomerization may be achieved via intermolecular excited-state double (or multiple) proton transfer (ESDPT) along intermolecular HBs acting as a proton-relay system. Among various hydrogen-bonded systems studied, such as dimers and alcohol and water complexes of 7-azaindole,[23−26] 1-azacarbazole,[27−29] 2-(2′-pyridyl)indole[30,31] and related compounds,[32,33] dipyrido[2,3-*a*:3′,2′-*i*]carbazole,[34−36] 1*H*-pyrrolo[3,2-*h*]-quinoline,[35−41] and PP,[42,43] a particular class of azaaromatic compounds—those mimicking the behavior of nucleic base pairs[44−46]—has attracted considerable interest. The mechanism of the excited-state double proton transfer (ESDPT) is being heavily discussed, in particular the issue of stepwise versus concerted movement of the protons.[10,47−49]

Recently, one of us proposed[50] a reversible optically driven molecular switch based on the mechanistic principles of the ESIPT phenomenon. The optical switch was composed of two covalently bound moieties: a molecular proton-donating/accepting "frame" (PDA) and a proton-accepting "crane", PA (Scheme 1). An important modification in comparison with typical ESIPT systems was that the molecular frame had not only a proton-donating group X−H but also a proton-accepting atom Z. On the other hand, the proton crane PA had only a single proton-accepting site Y. The optical excitation $S_1^{I} \leftarrow S_0^{I}$ of the tautomeric form **I** induced excited-state proton transfer ($PT^{I,IIa}$) along the hydrogen bond X−H···Y (i.e., from the X−H group of PDA to the Y site of PA), resulting in the structure **IIa**. The next step, which involved twisting around a covalent bond connecting PA and PDA (the double bond in the S_0 state is changed into nominally single bond in the excited $^{1}(\pi,\pi^*)$

Received: April 12, 2013
Revised: July 19, 2013
Published: August 21, 2013

   dx.doi.org/10.1021/jp403621p | *J. Phys. Chem. A* 2013, 117, 9127−9146

Scheme 1. Schematic Potential Energy Diagram, in the Form of a Cross-Section of the Energy Hypersurfaces along the Reaction Path, Illustrating the Idea of an Optically Driven Molecular Switch Composed of Two Moieties, a Molecular Frame (PDA) and a Proton "Crane" (PA)[51] (Explanation in Text)

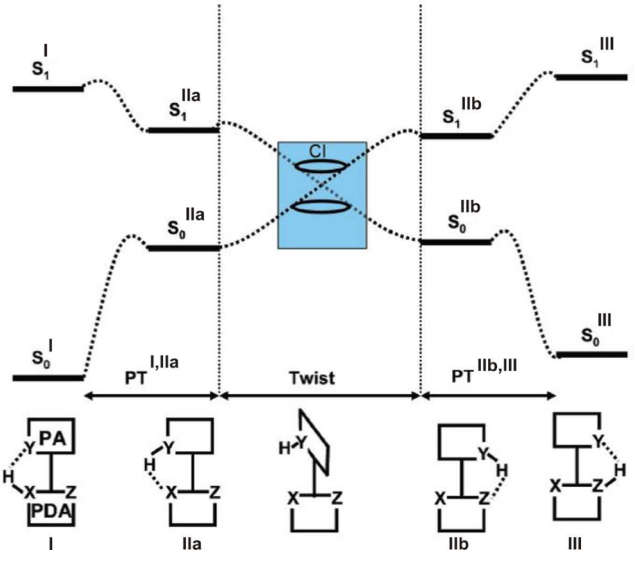

state S_1), led to a S_0–S_1 conical intersection region (CI). After $S_1 \rightarrow S_0$ nonadiabatic transition at the CI, the system could either return to the initial form **I** (the **IIa** form was theoretically predicted[50−53] to be not stable in S_0 and it relaxed spontaneously toward the form **I**) or continue the torsional motion leading to structure **IIb** (with a formation of the Y−H··· Z hydrogen bond). A second $PT^{IIb,III}$ process from the Y−H group of PA to the Z atom of PDA resulted in the tautomeric form **III**.

A computational study of the potential energy profiles along the relevant internal coordinates (such as the X−H and Y−H bond stretching distances, rotation around a single bond connecting PA and PDA moieties) suggested that the reversible ESIPT process could be observed for a series of molecules containing 7-hydroxyquinoline as the molecular "frame" and oxazine,[50,51] pyridine[51,52] (and other six-membered ring heterocycles[51]), and the carbaldehyde group[50,51] as the proton crane (Scheme 2). Among them, the carbaldehyde moiety seemed to be a reasonably good choice, being comparably small in size and lightweight, thus allowing for fast rotation, even when protonated. The reversible ESIPT process was observed, indeed, by irradiating the monomer of 7-hydroxy-4-methylquinoline-8-carbaldehyde (**H4MQC**), isolated in a low-temperature Ar matrix, with UV light of proper wavelengths.[53]

A similar molecular crane system, 7-hydroxy-8-(*N*-morpholinomethyl)quinoline, was studied 20 years ago by Varma and co-workers.[54] He proposed and confirmed the twisting one-way mechanism of the ESIPT process by the photostationary and time-resolved fluorescence investigations in solvents of various viscosity. The fluorescence behavior of **7HMMQ** (Figure 1) was compared with that of 2-hydroxy-1-(*N*-morpholinomethyl)naphthalene (2HMMN) and of **7-HQ**. In polar solvents **7HMMQ** showed, contrary to the other compounds, three fluorescence bands. Two bands, at the short- and long-wave sides of the spectrum, were also observed in the fluorescence spectrum of **7-HQ** in alcohols. These two bands

Scheme 2. Structures of Isomeric Forms of H4MQC and Schematic Representation of the Photoprocesses Interconverting the Tautomers I (OH, 7-Quinolinol), IIa, IIb, and III (NH, 7(1*H*)-Quinolinone, Whose Resonance Hybrid Is the Zwitterion Z)[a]

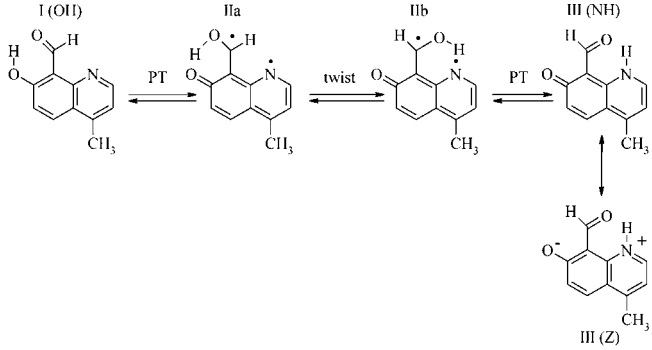

[a]The **IIa** and **IIb** structures correspond to the excited-state forms of biradical nature.

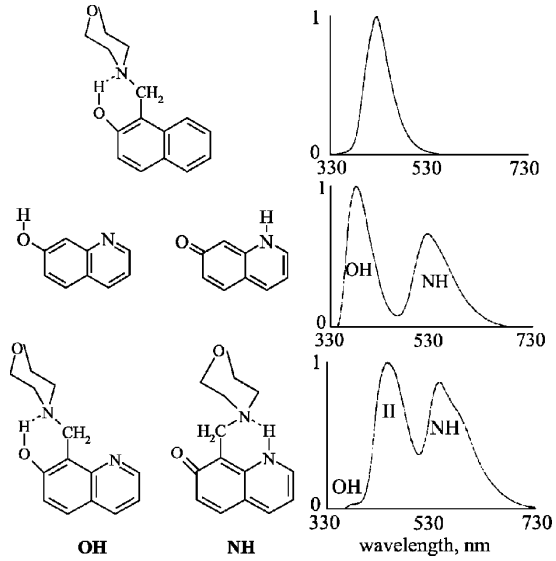

Figure 1. Molecular structures (left) and corresponding fluorescence spectra (right) of 2-hydroxy-1-(*N*-morpholinomethyl)naphthalene in acetonitrile (top), 7-hydroxyquinoline in methanol (middle), and 7-hydroxy-8-(*N*-morpholinomethyl)quinoline in acetonitrile (bottom) at room temperature (as inferred from ref 54). **OH**, **NH**, and **II** denote the neutral tautomeric forms; **II** is the transient intermediate form in the ESIPT process. See text for explanation.

were assigned to emissions from the primary excited **OH** tautomeric form and the adiabatically produced excited **NH** form, respectively. The third band originated from an excited transient species **II** (when the proton was located at the N atom of the morpholine moiety). The proposed mechanism of the excited-state long-range intramolecular phototautomerization of **7HMMQ** was as follows: a morpholinomethyl side group (proton crane) picked up the proton from the initial point on one side (OH group) of the frame moiety and deposited it at the final point (nitrogen atom) on the opposite side. The twisting mechanism was confirmed by time-resolved fluorescence investigations in solvents of various viscosity.[54] A substantial difference between this mechanism and that proposed in refs 50−53 is that the reverse ESIPT reaction is impossible for **7HMMQ** because the "saturated" molecular

dx.doi.org/10.1021/jp403621p | J. Phys. Chem. A 2013, 117, 9127−9146

crane (morpholinomethyl) precludes the presence of the S_1-S_0 conical intersection, which is essential for reversibility of the reaction.

Tautomerization of 7-hydroxyquinoline (**7-HQ**) was a subject of intense investigations. For the ground[55−59] and excited-state[60,61] prototropic reactions of the neutral tautomeric forms **OH** (7-quinolinol) and **NH** (7(1*H*)-quinolinone, the tautomer having as its resonance hybrid a zwitterionic species **Z**, Scheme 2) and the ionic species, the protonated cation (**C**) and the deprotonated anion (**A**) have been studied using steady-state UV−vis,[55,56,58,59] IR,[57] and fluorescence experiments,[60,61] as well as time-resolved techniques.[62−69] Mason et al.[60] concluded that in the excited state the hydroxyl group is more acidic and the ring nitrogen atom more basic than in the ground state. It is a "driving force" for the ESIPT reaction.

In **7-HQ** the acidic hydroxyl group and the basic nitrogen atom in the ring are too far apart to form an intramolecular hydrogen bond. Thus, the phototautomerization of **7-HQ** was observed only in protic solvents (e.g., alcohols) and took place via a triple proton-transfer process in hydrogen-bonded 1:2 solute−solvent complexes.[62−69] Thistlethwaite and Corkill[62,63] were the first to determine the reaction rate for the overall proton-transfer process of **7-HQ** in methanol, using time-resolved fluorescence measurements. From the rise-time of the long-wave fluorescence assigned to the **NH** tautomer they concluded that the process takes place in ca. 170 ps. In 1983 Itoh et al.[64] reported the detection of the metastable ground-state **NH** tautomer in methanol by transient absorption spectroscopy. They found that the excited-state tautomerization in methanol occurred within ca. 170 ps, but the ground-state process required at least 3.5 μs at room temperature. A study of the intensity of the long-wave fluorescence band as a function of methanol concentration in a mixture of *n*-hexane and methanol indicated that two alcohol molecules are involved in the ESPT process of **7-HQ**.[66] This picture was confirmed by Varma et al.,[67] who suggested that the tautomerization is restricted to a particular complex, most probably of a cyclic structure, and considered a two-step model for the tautomerization of **7-HQ**. They reported biexponential rise signals of the long-wave fluorescence and assigned a fast component (minor) to a direct ESPT in a cyclic 7HQ·(alcohol)$_2$ complex and the slow one (major) to a two-step process wherein the solvated 7HQ·(alcohol)$_n$ complex was thermally reorganized to a cyclic intermediate in the excited state, which was followed by ESPT (Scheme 3). The investigations of 1:2 complexes of **7-HQ** in mixed *n*-hexane solutions containing small amount of alcohol have shown that the rate constant of ESPT is correlated with the acidity of the alcohols.[69] The formation of water-chain complexes of 1:2 and 1:3 stoichiometry has been proved by investigations of **7-HQ** complexes isolated under supersonic jet conditions.[70,71] The formation of hydrogen-bonded 7-HQ·(methanol)$_n$ (n = 1, 2) and 7-HQ·$(H_2O)_n$ (n = 1−3) complexes and predicted multiple proton transfer has been investigated by Fang by means of ab initio computations.[72,73]

The mechanism of the ESPT process in aqueous solutions seems to be more complex than in alcohols; the excited-state tautomerization is reported to proceed in a stepwise fashion via forming anionic intermediate species.[68,74−78] Moreover, it is possible that two different rotamers of *trans*-**7-HQ** and *cis*-**7-HQ** affect the ESPT process of **7-HQ** as well.[78−80]

The problems discussed in this paper concern the solvent-dependent ground- and excited-state tautomerization in the custom-designed series of 7-hydroxyquinoline-8-carbaldehydes

Scheme 3. Solvent-Assisted Excited-State Proton Transfer (ESIPT) of 7-Hydroxyquinoline (7-HQ) in Alcohols, as Inferred from Ref 67 (Explanation in Text)

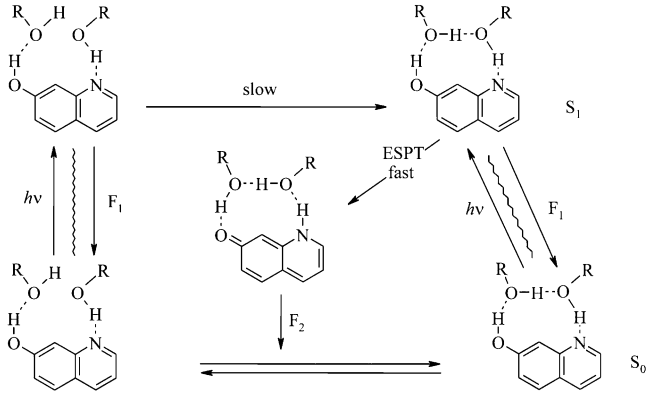

(**7-HQCs**) [7-hydroxyquinoline-8-carbaldehyde (**HQC**), 7-hydroxy-2-methylquinoline-8-carbaldehyde (**H2MQC**), 7-hydroxy-4-methylquinoline-8-carbaldehyde (**H4MQC**), 7-hydroxy-2,4-dimethylquinoline-8-carbaldehyde (**HDMQC**), 7-hydroxy-2-methoxy-4-methylquinoline-8-carbaldehyde (**HMMQC**), 7-hydroxy-2-phenylquinoline-8-carbaldehyde (**HPQC**), 7-hydroxy-2-(2′-methylphenyl)quinoline-8-carbaldehyde (**HMPQC**)], as well as respective molecular frame models [7-hydroxyquinoline (**7-HQ**), 7-hydroxy-2-methylquinoline (**H2MQ**), 7-hydroxy-4-methylquinoline (**H4MQ**), 7-hydroxy-2,4-dimethylquinoline (**HDMQ**), 7-hydroxy-2-methoxy-4-methylquinoline (**HMMQ**), 7-hydroxy-2-phenylquinoline (**HPQ**), 7-hydroxy-2-(2′-methylphenyl)quinoline (**HMPQ**)] (Scheme 4). The effects of temperature, polarity, and hydrogen-bonding ability of the environment on the ground- and excited-state equilibria, as well as on the spectroscopic and photophysical properties of the solute (e.g., quantitative characterization of the electronic structure, excited-state dipole moments, and radiative and radiationless transitions and the resulting structural changes), are examined and discussed. Moreover, the aim of this work is to study the effects of the position of a substituent (in terms of its electron-withdrawing and -donating properties) on the spectroscopy and luminescence properties of these **7-HQCs**, as well as on their photostability.

The spectroscopic and photophysical properties of the compounds in aqueous solutions and prototropic equilibria are presented and discussed in part 2.[81]

2. METHODS

2.1. Experimental Section. *Synthesis, Purification, and Identification of the Compounds.* 7-Hydroxyquinoline-8-carbaldehyde (**HQC**) and its derivatives (**H2MQC**, **HDMQC**, **HMMQC**, **HPQC**, **HMPQC**) were prepared in moderate yields from 7-hydroxyquinolines (**7-HQs**) by Reimer−Tiemann reaction according to the procedure described in ref 53. for the synthesis of **H4MQC**. Respective 7-hydroxyquinolines (**7-HQ**,[82] **H2MQ**,[83] **HDMQ**,[84] **HPQ**,[85] and **HMPQ**[85]) were synthesized following literature methods, except for **HMMQ**, which was obtained by reacting 2-chloro-7-hydroxy-4-methylquinoline[53] with sodium methoxide. The newly obtained hydroxyquinoline carbaldehydes (**7-HQCs**), along with the simplest of them 7-hydroxyqunoline-8-carbaldehyde (**HQC**) (synthesis described in ref 86 where only melting point and elemental analysis is reported) and 7-

dx.doi.org/10.1021/jp403621p | J. Phys. Chem. A 2013, 117, 9127−9146

Scheme 4. Labeling of Atoms and Acronyms of the Investigated 7-Hydroxyquinoline-8-carbaldehydes (HQC, H4MQC, H2MQC, HDMQC, HMMQC, HPQC, HMPQC) and Respective 7-Hydroxyquinolines (7-HQ, H4MQ, H2MQ, HDMQ, HMMQ, HPQ, HMPQ)[a]

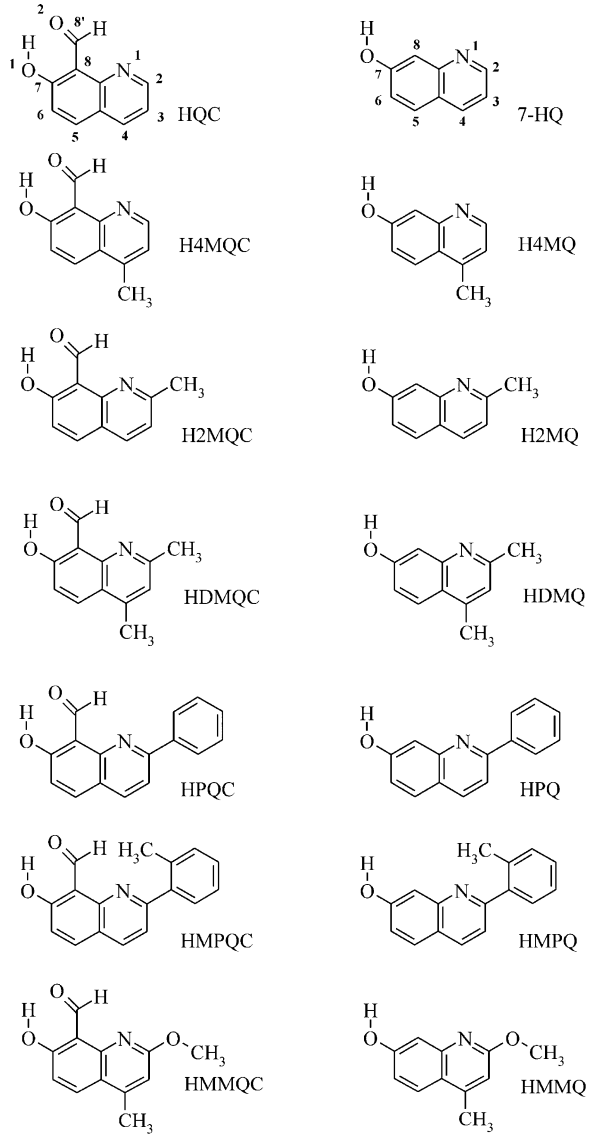

[a]O_1, O_2, and $C_{8'}$ atoms were numbered arbitrarily for the purpose of description of the $C_7C_8C_{8'}O_2$ torsional angle. See text for full names.

HQ derivatives were characterized by their melting points, ^{1}H and ^{13}C NMR spectra, and HR-MS. Proton and carbon NMR spectra (registered in deuterated methanol) are also reported for the **NH** form of **HDMQC**: 8-formyl-2,4-dimethyl-1*H*-quinolin-7-one (see Supporting Information).

All the **7-HQs** and **7-HQCs** were crystallized from methanol−methylene chloride or methylene chloride and hexane−methylene chloride or methylene chloride, respectively. Melting points were uncorrected. ^{1}H and ^{13}C NMR spectra were recorded on a Varian UNITYplus-200 instrument. Mass spectrometry was performed on an AMD 604 with an EI 70 eV ionization source.

Solvents Used for Our Studies. *n*-Hexane (HEX), ethyl acetate (EA), acetonitrile (ACN), liquid paraffin, and the alcohols: methanol (MeOH), 1-propanol (1-PrOH), and 1-butanol (1-BuOH) were of spectroscopic or fluorescence grade (Aldrich or Merck). Butyronitrile, BN (Merck, for synthesis), was distilled successively over $KMnO_4$ + K_2CO_3, P_2O_5, and CaH_2. Water was used after four distillations over $KMnO_4$ in a quartz apparatus. The solvents were selected to cover a wide range of the static permittivity values ε (HEX, EA, BN, ACN),[87] as well as the value of the index α describing the solvent hydrogen bond donor ability of bulk water and alcohols.[88] All solvents were checked for the presence of fluorescing impurities. NMR studies were performed in the following deuterated solvents (99.8% D, ARMAR Chemicals and Cambridge Isotope Laboratories, Inc.): perdeuterated cyclohexane, dichloromethane (CD_2Cl_2), chloroform ($CDCl_3$), acetonitrile (CD_3CN), and methanol (CD_3OD).

Instrumentation and Procedures. Electronic absorption spectra were obtained on Shimadzu UV 2401 and Shimadzu UV 3100 spectrophotometers. The latter was equipped with variable-temperature chamber. Stationary fluorescence and fluorescence excitation spectra were measured on an Edinburgh FS 900 CDT fluorometer and with the Jasny multifunctional spectrofluorometric system.[89] The spectra were corrected using the spectral sensitivity curves of the instruments. Fluorescence spectra were recorded as a function of wavelength (λ) and subsequently multiplied by a factor of λ^2 to convert counts per wavelength into counts per wavenumber. For the quantum yield determinations, the solutions had identical optical densities at the excitation wavelength. Quinine sulfate in 0.05 mol dm^{-3} H_2SO_4 (ϕ_f = 0.51)[90] served as reference for fluorescence quantum yield determination. Fluorescence lifetimes were measured on an Edinburgh FL 900 CDT time-resolved fluorometer, with an estimated time resolution of about 500 ps. The time-resolved single photon counting technique was used, followed by data reconvolution using nonlinear least-squares fitting routine. For a temporal resolution better than 500 ps a home-built setup was used, with a Picoquant picosecond laser, emitting at 379 nm, and a Becker & Hickl SPC-830 single photon detection module.

NMR spectra were recorded on a Bruker Avance II 300 spectrometer operating at 300.17 MHz for ^{1}H with a BVT-3200 variable-temperature unit. The temperature ^{1}H NMR studies were performed in three solvents: acetonitrile-d_3, $CDCl_3$ and CD_2Cl_2 in the range of temperatures from 298 to 213 K (in the case of acetonitrile down to 233 K). Concentration of the NMR samples was 7 mM. They were prepared either in a drybox from freshly deuterated solvents (acetonitrile, CD_2Cl_2) or by distillation in a vacuum line ($CDCl_3$ dried with CaH_2). Five millimeter glass NMR tubes were sealed under argon to avoid condensation of water from air. The experiments in which samples were irradiated with UV light prior to recording NMR spectra were carried out on 2 mM solution in CD_3CN and 7 mM solution in $CDCl_3$. The UV irradiation at wavelengths above 365 nm was performed outside the spectrometer, directly in sealed NMR tubes through glass walls with a Hg-lamp.

2.2. Computational Methods and Procedures. The ground-state equilibrium geometries of all the molecular systems, in either their neutral or ionic (protonated or deprotonated) state, were determined with the MP2 method. Excitation energies and response properties were calculated with the CC2 method,[91,92] a simplified and computationally efficient version of the coupled-cluster method with singles and doubles (CCSD). The equilibrium geometries of the lowest excited singlet states was determined at the CC2 level, making use of the CC2 analytic gradients.[93,94] Dunning's correlation-

dx.doi.org/10.1021/jp403621p | J. Phys. Chem. A 2013, 117, 9127−9146

consistent split-valence double-ζ basis set with polarization functions on all atoms (cc-pVDZ)[95] was employed in these calculations. To better reproduce the UV absorption spectrum, the S_0-equilibrium geometries were reoptimized with the aug-cc-pVDZ[95] basis set augmented with the diffuse functions. For these geometries the vertical excitation energies were calculated at the CC2/aug-cc-pVDZ level.

To estimate barriers for the photophysically relevant reactions in the ground-state S_0 and in the lowest excited singlet states, $^1(n,\pi^*)$ and $^1(\pi,\pi^*)$, the minimum-energy reaction paths (solid curves in Figures 11 and 12) were determined by MP2 and CC2 methods, respectively, using the cc-pVDZ basis set. For a suitably chosen driving coordinate, all other nuclear degrees of freedom were optimized for a given value of the driving coordinate, the internal coordinate most closely resembling the desired reaction coordinate. The three different driving coordinates were applied, which, on three separate panels, described a three-part photoswitching mechanism: (i) the O_1H bond length for the **I** (**OH**) ↔ **IIa** proton transfer (shown in panels a), (ii) the $C_7C_8C_{8'}O_2$ dihedral angle (twisting of the carbaldehyde group with respect to the quinoline ring) for the reaction path connecting the **IIa** and the **IIb** forms (shown in panels b), and (iii) the N_1H distance for the **IIb** ↔ **III** (**NH**) proton transfer (shown in panels c).

In addition, the potential-energy profiles of the S_0 state calculated at the optimized geometry of the given excited state, $S_0(\pi,\pi^*)$ and $S_0(n,\pi^*)$, are shown (dashed curves) to indicate the proximity of the S_0 state to the profile of a given excited state, $^1(n,\pi^*)$ or $^1(\pi,\pi^*)$, and thus to estimate the fluorescence energy corresponding to the given excited-state minimum or to predict a fast nonradiative channel through the CI region.

To check the influence of the solvent (in comparison to vacuum conditions) on the relative stability of the ground-state tautomeric forms of the **HQC** and **HMMQC**, additional single-point-MP2 calculations in conjunction with the polarizable continuum model (PCM)[96,97] with the aug-cc-pVDZ basis set were done, simulating water and acetonitrile environments, at the geometries optimized at the MP2/aug-cc-pVDZ level.

All MP2 and CC2 calculations were carried out with the TURBOMOLE program package,[98] making use of the resolution-of-the-identity (RI) approximation for the evaluation of the electron-repulsion integrals.[99] The PCM/MP2 calculations were performed with the Gaussian 09 program package.[100]

Density functional theory (DFT) and time-dependent DFT (TD DFT) computations were performed using Gaussian 03[101] and Gaussian 09[100] suites of programs. The B3LYP (Becke, Lee, Yang, and Parr three-parameter)[102−104] hybrid functional with 6-31+G(d,p) basis set were applied in both cases.

3. RESULTS AND DISCUSSION

3.1. Ground-State Tautomerization: Electronic Absorption, NMR Studies, and Theoretical Computations.

Theoretical Predictions. All the experimentally studied compounds were investigated theoretically with the aid of electronic-structure methods in their ground and lowest electronically excited singlet states $^1(\pi,\pi^*)$ and $^1(n,\pi^*)$. The stable forms for these electronic states were optimized and their spectroscopic properties were analyzed with respect to the absorption and fluorescence spectra to help in assignment and interpretation of experimental data. The ab initio computed transition energies of the respective tautomeric and rotameric forms of the studied compounds are collected in Tables S1−S12 (Supporting Information), whereas the fluorescence energies for the respective excited-state forms are collected in Table S13 (Supporting Information). The photophysically relevant potential-energy profiles (corresponding to Scheme 1) of two selected compounds: **HQC** and **HMMQC** are presented in Figures 11 and 12.

Electronic Absorption. The room-temperature electronic absorption spectra of **7-HQCs** and **7-HQs** were recorded in nonpolar (*n*-hexane), medium polar aprotic (ethyl acetate), strongly polar aprotic (acetonitrile), and polar protic (1-propanol, methanol, water) solutions. The near-UV absorption spectrum (Figure 2, Table 1) of **HQC** in *n*-hexane shows three

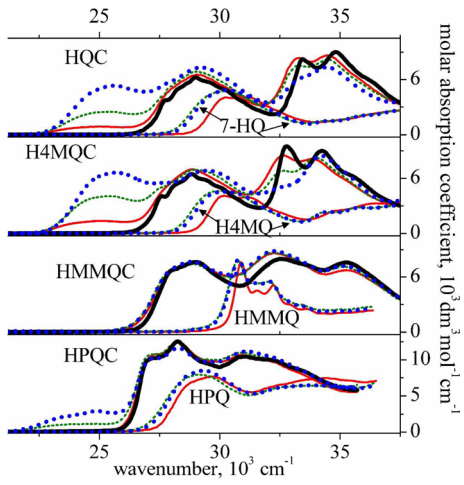

Figure 2. Comparison of the room-temperature absorption spectra of **7-HQCs** and corresponding **7-HQs**: full thick lines (black), *n*-hexane; full thin lines (red), acetonitrile; dotted thin lines (green), 1-propanol; dotted thick lines (blue), methanol. The spectra of **H2MQC** and **HDMQC** are similar to those of **H4MQC**, and spectra of **HMPQC** are similar to those of **HPQC**. The solubility of **7-HQs** in *n*-hexane is too low to determine the molar absorption coefficients.

bands centered at ∼345, 299, and 287 nm (∼29000, ∼33450, and ∼34850 cm^{-1}, respectively). These bands do not reveal any significant shift with increasing solvent polarity. On the other hand, the increase of solvent polarity and its hydrogen-bonding ability leads to the appearance of a low-energy band at ca. 400 nm (∼25000 cm^{-1}). This long-wave band is particularly intense in strongly polar and protic environments, such as methanol and water (see part 2[81]).

Similar solvent effects on the absorption spectra are observed for the other **7-HQCs** under study, except **HMMQC** (see below). Interestingly, the intensity of the low-energy band observed for **HPQC** is lower than that of **HQC** and its methyl substituted derivatives. According to the previous results of the experimental investigations of **H4MQC** in low-temperature matrices[53] and the results of calculations,[50,51] we suppose that both forms, **OH** and **NH** (Scheme 2), are present already in the ground state. The ab initio CC2/cc-pVDZ computations predict that the vertical excitation energies to the lowest $^1(\pi,\pi^*)$ states of the **NH** forms are about 25000 cm^{-1} (for **HQC** and its methylated derivatives) and 23250 cm^{-1} (**HPQC**) under vacuum conditions (Table 2, Tables S1−S6, Supporting Information). These spectral positions are lower by ca. 7000 and 5400 cm^{-1} than those predicted for the **OH** and **IIb** forms, respectively. The structure **IIa** is predicted to be generally not stable in the ground electronic state as it relaxes

dx.doi.org/10.1021/jp403621p | J. Phys. Chem. A 2013, 117, 9127−9146

Table 1. Solvent Effects on the Spectral Positions of Room-Temperature Electronic Absorption Maxima (λ_{abs}, nm),[a] Molar Absorption Coefficients (ε, dm^3 mol^{-1} cm^{-1}), and Electronic Transition Dipole Moments (M_{abs}, D,[b] Eq S4, Supporting Information) Assigned to the OH and NH Tautomeric Forms of 7-HQCs and 7-HQs (Explanation in Text)

		7-HQCs					7-HQs[c]			
	solvent	λ_{abs} OH	ε	λ_{abs} NH	ε	M_{abs} OH	λ_{abs} OH	ε	λ_{abs} NH	M_{abs} OH
HQC/7-HQ	HEX	345	6500			2.2				
	EA	345	6120			2.1	331	4100		1.7
	ACN	344	6530	400	~9700		331	4000		1.7
	1-PrOH	345	6980	395			331	4700		1.9
	MeOH	343	7360	390	~10500		331	4800		1.9
H4MQC/H4MQ	HEX	347	6350			2.1				
	EA	347	6100			2.0	333	3900		1.7
	ACN	347	6990	400	~9000		333	4100		1.7
	1-PrOH	345	6890	395			333	4600		1.8
	MeOH	340	7170	390	~10800		333	4550		1.9
H2MQC/H2MQ	HEX	344	5700				327			
	EA	344	6390				330	4900		1.9
	ACN	344	6740	400			328	5100		1.9
	1-PrOH	345	7190	400			330	5800		2.0
	MeOH	345	9120				330	5650		2.1
HDMQC/HDMQ	HEX	348	~7300							
	EA	345	7290				330	6300		2.0
	ACN	348	7720	395			330	6750		2.1
	1-PrOH	346	8210	385			330	7800		2.4
	MeOH	345	8470	390	~12900		330	7300	~400	2.3
HPQC[d] **/HPQ**	HEX	354	12530				333			
							345			
	EA	354	12920				338	7500		2.3
	ACN	354	12430	420			338	7700		2.4
	1-PrOH	354	12420	420			342	7900		2.3
	MeOH	354	11720	400			342	8500		2.5
HMPQC/HMPQ	HEX	350	9300							
	EA	350	10000				332	6900		2.1
	ACN	350	9650				332	6200		2.0
	1-PrOH	350	9600	410			337	7600		2.2
	MeOH	350	9220	400			335	7100		2.1
HMMQC/HMMQ	HEX	346	7690			2.4	323			
	EA	346	7570			2.4	324.5	8200		1.9
	ACN	346	7560			2.4	323.5	7600		1.8
	1-PrOH	346	7630			2.4	325.5	7800		1.9
	MeOH	346	7660			2.5	325	7900		2.0

[a]Scatter of results: ±2.0 nm. [b]Estimated error: 10%. [c]The solubility of **HQC**, **H4MQC**, **HDMQC**, and **HMPQC** in *n*-hexane is too low to measure the absorption spectra. [d]There are two electronic absorption maxima of the **OH** form centered at ~354 and ~369 nm. Theoretical TD-DFT/B3LYP/6-31+G(d,p) computations (Table 2) predict that the maxima correspond to two lowest $^1(\pi,\pi^*) \leftarrow S_0$ transitions.

spontaneously toward the **OH** form. The TD-DFT/B3LYP/631+G(d,p) computations (Table 2) show similar results; the calculated values are lower (as expected) than those obtained with the ab initio CC2/cc-pVDZ method. Thus, the long-wave absorption band can be assigned to the **NH** tautomer. The computed values of dipole moments support this assignment. The calculations predict that the **OH** form should be dominant in the ground state for all the studied molecules under vacuum conditions (Table 3). The calculated energy gap ΔE between **OH** and **NH** forms is about 6 kcal/mol (DFT calculations) and 11 kcal/mol (MP2) for **HQC**, its methylated derivatives, and **HPQC**. The dipole moments of the **NH** tautomers of all the **7-HQCs** under study are about two times higher than those of the **OH** forms (Table 3; Tables S1−S6, Supporting Information). This should favor the stabilization of the **NH** form in polar solvents, which is indeed observed as the appearance and growth of the low-energy band in absorption.

In protic solvents another factor that can change the relative energies of the **OH** and **NH** forms is the influence of intermolecular hydrogen bonds on their stabilization energies. Noticeably, although the MP2/aug-cc-pVDZ simulations of the solvent effect (with the use of the PCM model)[96,97] on the relative energies of the tautomeric forms of **HQC** (and **HMMQC**) do not show any significant differences between acetonitrile and water (Table S14, Supporting Information), the incorporation of the discrete model (Table 6) leads to the substantial stabilization of the 1:2 complexes of the **NH** form.

Contrary to the other **7-HQCs** under study, the electronic absorption spectra of **HMMQC** do not show the long-wave band centered at about 400 nm even in acetonitrile and alcohols (Figure 2). Therefore, the bands observed at about 346, 305, and 284 nm (~29000, ~32600, and ~35250 cm^{-1}, respectively) are assigned to the **OH** form. On the other hand, a relatively small increase of the intensity is observed at the red

dx.doi.org/10.1021/jp403621p | J. Phys. Chem. A 2013, 117, 9127−9146

Table 2. Comparison between Vertical ab Initio CC2/cc-pVDZ ($\tilde{\nu}_{CC2}$, 10^3 cm^{-1}) and TD-DFT B3LYP/6-31+G(d,p) ($\tilde{\nu}_{TDDFT}$) Excitation Energies of the Low-Lying $^1(\pi,\pi^*) \leftarrow S_0$ Transitions and Oscillator Strengths (f_{CC2}, f_{TDDFT}) for Various Forms (Scheme 1) of HQC, H4MQC, HPQC, and HMMQC and the Locations of the Experimental Absorption Maxima ($\tilde{\nu}_{exp}$, Scatter of Results: ±150 cm^{-1}) in *n*-Hexane[a]

compound	tautomer	excited state	$\tilde{\nu}_{CC2}$	f_{CC2}	excited state	$\tilde{\nu}_{TDDFT}$	f_{TDDFT}	$\tilde{\nu}_{exp}$
HQC	**I (OH)**	S_2	32.10	0.117	S_2	30.75	0.103	~29.0
		S_3	38.23	0.093	S_4	34.21	0.075	33.45
		S_4	40.33	0.056	S_5	37.00	0.098	34.85
	III (NH)	S_2	25.25	0.130	S_2	24.61	0.100	25.00
		S_3	31.05	0.192	S_4	30.22	0.115	
		S_4	38.80	0.034	S_7	35.13	0.073	
	IIb	S_2	30.57	0.179	S_2	28.29	0.131	
		S_3	33.63	0.082	S_3	31.33	0.027	
		S_4	40.97	0.243	S_6	36.98	0.265	
H4MQC	**I (OH)**	S_2	31.86	0.114	S_2	30.46	0.103	~28.8
		S_3	37.75	0.132	S_3	33.51	0.117	32.8
		S_4	40.65	0.032	S_5	37.25	0.059	34.28
	III (NH)	S_2	24.68	0.120	S_2	24.24	0.094	25.33
		S_3	30.97	0.194	S_4	30.25	0.108	28.6[b]
		S_4	38.39	0.062	S_6	35.13	0.107	
	IIb	S_2	30.00	0.174	S_2	27.87	0.129	
		S_3	33.72	0.065	S_6	36.52	0.318	
		S_4	40.17	0.301	S_8	41.16	0.053	
HPQC	**I (OH)**	S_2	30.65	0.221	S_2	28.47	0.304	~27.1
		S_3	34.92	0.239	S_3	30.55	0.070	28.23
		S_4	38.15	0.020	S_5	33.68	0.019	31.0
	III (NH)	S_2	23.23	0.223	S_2	22.77	0.111	23.74
		S_3	30.41	0.157	S_4	29.49	0.087	28.3[b]
		S_4	35.01	0.277	S_6	31.95	0.221	
	IIb	S_2	29.20	0.317	S_2	26.90	0.262	
		S_3	32.02	0.066	S_3	29.61	0.021	
		S_4	36.30	0.436	S_4	33.06	0.293	
HMMQC	**I (OH)**	S_2	31.86	0.159	S_2	29.63	0.114	~29.0
		S_3	36.46	0.123	S_3	32.76	0.114	~32.6
		S_4	39.85	0.089	S_4	37.12	0.125	~35.25
	III (NH)	S_2	26.94	0.231	S_2	26.49	0.174	
		S_3	29.36	0.169	S_3	28.65	0.099	
		S_4	39.20	0.058	S_6	36.04	0.091	
	IIb	S_2	29.44	0.188	S_2	26.66	0.112	
		S_3	33.31	0.130	S_3	31.68	0.088	
		S_4	38.64	0.278	S_5	35.99	0.302	

[a]Only transitions of significant intensity are shown ($f > 0.02$). [b]$\tilde{\nu}_{exp}$ obtained from the excitation spectra in ACN (Figures 4 and 6).

Table 3. Ground-State MP2/cc-pVDZ (ΔE_{MP2}) and DFT/B3LYP/6-31+G(d,p) (ΔE_{DFT}) Relative Energies (kcal mol^{-1}) of the OH, NH, and IIb forms (Scheme 2) of HQC, H4MQC, HPQC, and HMMQC in a Vacuum and the Corresponding Dipole Moments (μ, D)

		I (OH)		III (NH)		IIb	
		ΔE_{MP2}	ΔE_{DFT}	ΔE_{MP2}	ΔE_{DFT}	ΔE_{MP2}	ΔE_{DFT}
HQC	ΔE			11.3	6.2	9.9	7.8
	μ	3.5	5.0	6.6	8.0	4.7	5.8
H4MQC	ΔE			11.5	6.2	10.1	7.7
	μ	4.0	5.6	7.1	8.7	5.1	6.4
HPQC	ΔE			10.8	5.9	9.7	7.8
	μ	3.3	4.9	7.2	8.7	5	6.2
HMMQC	ΔE			17.3	12.2	12.7	10.7
	μ	3	4.4	6.8	8.1	4.7	5.7

corner of the lowest absorption band with the increase of polarity and hydrogen bond donor and acceptor ability of the environment. This finding can be explained by an appearance of a very small fraction of the **NH** tautomeric form in polar media. The explanation is in agreement with the predicted vertical excitation energy to the lowest $^1(\pi,\pi^*)$ state of ca. 26500−27000 cm^{-1} in the **NH** form of **HMMQC**, which is about 2000 cm^{-1} higher than that computed for **HQC** and its methylated derivatives, and about 3700 cm^{-1} higher than that for **HPQC** (Table 2 and Tables S1−S6, Supporting Information).

The assignment of the absorption bands of the **7-HQCs** centered at about 29000 and 31000−34000 cm^{-1} (Figure 2) is more ambiguous due to the fact that close-lying electronic transitions are computed in this spectral region for the forms **OH**, **NH**, and **IIb** (Table 2, Tables S1−S6, Supporting Information). Noticeably, the predicted relative energies of the **IIb** forms of **7-HQCs** are similar to those of the **NH** tautomers (the computed destabilization energy of the **IIb** form of **HMMQC** is lower than that of the **III** form (Table 3, Table S14, Supporting Information). Thus, it is difficult to predict which tautomeric forms contribute to the experimental

dx.doi.org/10.1021/jp403621p | J. Phys. Chem. A 2013, 117, 9127−9146

absorption spectrum at this region. The evidence that only the **OH** and **NH** tautomers exist in the ground state is provided by the results of NMR investigations.

The electronic absorption spectra of **7-HQs** are significantly blue-shifted in comparison to the spectra of the corresponding **7-HQCs** (Figure 2, Table 1). The spectral positions of the lowest energy band of all the **7-HQs** do not depend on solvent properties and are centered at about 30000 cm^{-1}. The compounds (except **HDMQ** in methanol solutions) do not show any trace of the low-energy band. This finding indicates that the studied **7-HQs**, similarly to **7-HQ**,[55] in nonpolar and polar aprotic media, as well as in alcohols exist in the ground state as the **OH** (7-quinolinol) form.

NMR Investigations. The ^1H NMR investigations of **7-HQCs** were performed to identify the tautomeric forms that exist in the ground state. The spectra exhibit, in most cases, two sets of signals that can be ascribed to two forms of the same compound being in slow-exchange equilibrium (the upper limit of the conversion reaction rate was estimated as 10 s^{-1} at 298 K). The hydroxy and NH bridging protons are deshielded and exhibit NMR signals in the range 12−16 ppm. The chemical shifts in the range 10−12 ppm are characteristic for aldehydes. Thus, the observed chemical shifts strongly suggest the coexistence of the **OH** and **NH** tautomers for **HQC** and its derivatives in moderately polar (such as $CDCl_3$), polar (CD_3CN), and protic (CD_3OD) solvents. The evidence that one of the signals corresponds to the **NH** form is provided by line shape analysis. For **H4MQC** in CD_3CN, as an example, the signal at 15.2 ppm is broadened and exhibits two shoulders (Figure 3). This is clearly caused by the coupling to the ^{14}N

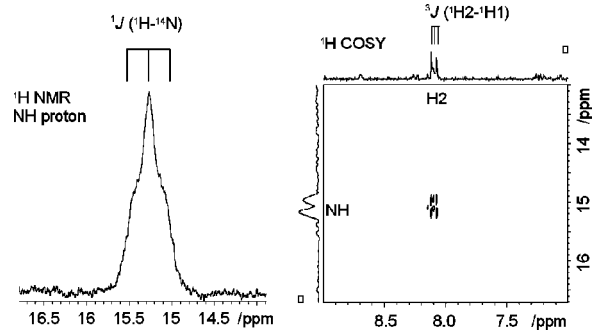

Figure 3. ^1H NMR signal of NH proton of **H4MQC** in CD_3CN showing coupling to the ^{14}N nuclei (left) and a cross-peak between NH and H2 proton signals of **H4MQC** (right). ^1J ($^1H-^{14}N$) ≈ 54 Hz, $^3J(^1H2-^1HN)$ = 6.3 Hz.

nuclei in the quinoline ring. The large value obtained for the coupling ^1J ($^1H-^{14}N$) ≈ 54 Hz is possible only for the direct H−N coupling through one bond. This fact excludes the origin of the line from the proton, which is hydrogen-bonded to the N quinoline atom as in the **IIb** structure (Scheme 2). Moreover, a 2D NMR COSY experiment shows a cross peak between H2 and HN protons and the coupling constant is 6.3 Hz. This is again a typical value for the ^3J ($^1H-^1H$) in an aromatic ring, which gives the next argument for the origin of this line from the **NH** form. These findings prove that the **NH** tautomer exists in solutions.

The estimated fractions of the **OH** and **NH** forms (Table 4) confirm the assignment of the electronic absorption bands. In a nonpolar solvent (perdeuterated cyclohexane) the NMR spectra of **H4MQC** indicate the lack of the **NH** form. Thus, the absorption band in *n*-hexane centered at 347 nm (~28820 cm^{-1}) corresponds to the **OH** tautomer. In moderately polar solvents (e.g., in ethyl acetate) the recorded trace of the long-wave absorption band of the all **7-HQCs** (except **HMMQC**) clearly corresponds to the appearance of the **NH** form observed in NMR experiments (in $CDCl_3$). Moreover, the increase of the intensity of the long-wave absorption band centered at about 400 nm (~25000 cm^{-1}) in acetonitrile and alcohols is related to the significant growth of the fraction of the **NH** form in strongly polar (CD_3CN) and protic (CD_3OD) media. Thus, there is no doubt that the long-wave absorption band corresponds to the **NH** tautomer.

The results of NMR investigations for **HMMQC** (Table 4) indicate that only a very small fraction of about 5% of the **NH** tautomer is formed in the ground state in strongly polar and protic media. This finding (which is in agreement with the results of calculations (Table 3; Tables S1−S6, Supporting Information): the predicted ground-state destabilization energy of the **NH** tautomer with respect to the **OH** form of **HMMQC** is about 1.5 (MP2) or 2 (DFT) times higher than that of the other **7-HQCs**) and the predicted vertical excitation energy of ca. 27000 cm^{-1} to the lowest $^1(\pi,\pi^*)$ state of the **NH** form of **HMMQC**) is in agreement with the lack of any considerable solvent effects on the electronic absorption spectra of this compound (Figure 2). These spectra in nonpolar and polar aprotic media, as well as in alcohols correspond to the **OH** form. Thus, **HMMQC** seems to be a good model to study the excited-state tautomerization process due to the fact that the **OH** tautomer (which is a substrate of the photoreaction) is a major form of the compound in the ground state in all solvents used for our studies.

3.2. Excited-State Long-Range Prototropic Tautomerization: Room and Low-Temperature Luminescence Investigations and Theoretical Computations. *Room-Temperature Studies of 7-HQCs.* The room-temperature fluorescence spectra of **HQC**, **H4MQC**, **H2MQC**, and **HMMQC** are presented in Figure 4. **HQC** and its methyl derivatives in acetonitrile and in alcohols show a single broad fluorescence band with a maximum centered at about 20500 cm^{-1} and at about 21000 cm^{-1}, respectively. The fluorescence excitation spectra (monitored for various parts of the fluorescence spectrum) show that luminescence is preferentially excited from the low-energy absorption band. The shape and spectral position of fluorescence recorded upon direct excitation of the **NH** form at 25000 cm^{-1} and upon excitation of the **OH** and **NH** forms at the second absorption band at 28570 cm^{-1} (Table 2 and Table S1, Supporting Information) are very similar. Therefore, it is natural to propose that fluorescence in sufficiently polar media originates from the **NH** tautomer.

On the contrary, the emission spectra of **HQC**, **H2MQC**, and **H4MQC** in *n*-hexane and in ethyl acetate exhibit two bands: a dominant emission at about 21000 cm^{-1} and a second one of lower intensity at 24000−24500 cm^{-1}. The spectra of **HDMQC** (not shown) are considerably wider than those in highly polar and protic media. These interesting spectral features demonstrate that the emission in nonpolar and medium polarity solvents originates from at least two different species. The spectral position of the long-wave fluorescence is similar to that observed in acetonitrile and in alcohols. Thus, this emission is assigned to the **NH** tautomer. The assignment of the short-wave emission is more ambiguous. Most probably, the **OH** tautomeric form (which dominates in the ground

dx.doi.org/10.1021/jp403621p | J. Phys. Chem. A 2013, 117, 9127−9146

Table 4. Ground-State Fractions of the OH (7-Quinolinol) and NH (7(1*H*)-Quinolinone) Tautomeric Forms of 7-HQCs Obtained from Room-Temperature ^{1}H NMR Spectra

	cyclohexane	$CDCl_3$	CD_3CN	methanol-d_4
HQC		**OH**, dominant; **NH**, trace	**OH**:**NH** ≈ 10:1[a]	**OH**:**NH** ≈ 1:1[a]
			91%:9%	50%:50%
H4MQC	100% **OH** (no **NH**)	**OH**:**NH** ≈ 10:1	**OH**:**NH** ≈ 5.5:1	**OH**:**NH** ≈ 1:1.6
		91%:9%	85%:15%	38%:62%
H2MQC		**OH**:**NH** ≈ 8:1		
		89%:11%		
HDMQC		**OH**:**NH** ≈ 4:1	**OH**:**NH** ≈ 5:1	**OH**:**NH** ≈ 1:2.7
		80%:20%	83%:17%	27%:73%
HPQC		**OH**, dominant; **NH**, trace	**OH**:**NH** ≈ 100:1	**OH**:**NH** ≈ 7:1
			99%:1%	87%:13%
HMPQC		**OH**, dominant; **NH**, trace		
HMMQC		100% **OH** (no **NH**)	**OH**:**NH** ≈ 20:1[a]	**OH**:**NH** ≈ 17:1[a]
			95%:5%	94%:6%

[a]Estimated from broad lines indicating faster exchange between two forms.

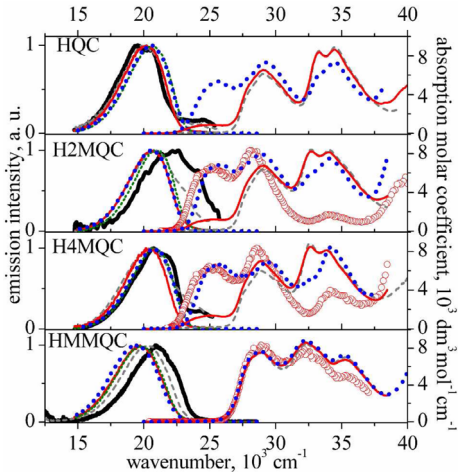

Figure 4. Room-temperature absorption and corrected and normalized fluorescence spectra (full thick lines (black), *n*-hexane; dashed thin lines (gray), ethyl acetate; full thin lines (red), acetonitrile; dotted thin lines (green), 1-propanol; dotted thick lines (blue), methanol) of **HQC**, **H2MQC**, **H4MQC**, and **HMMQC**. The emission spectra of **HDMQC** are similar to those of **H4MQC**. Concentrations of the compounds were in the range 10^{-5} to 10^{-4} mol dm^{-3}. Open circles (orange) are the fluorescence excitation spectra in acetonitrile monitored at the emission maximum.

state) is responsible for the emission observed at ∼24500 cm^{-1}. Interestingly enough, the shape of the fluorescence spectra of **H4MQC** (and **H2MQC**) suggests a third emission centered at 22100 (±500) cm^{-1}. This emission, similarly to the case of 7-hydroxy-8-(*N*-morpholinomethyl)quinoline (**7HMMQ**),[54,105] can be attributed to the transient intermediate structure **IIa** or **IIb** (Scheme 1). This interesting finding suggests that the **NH** tautomer, which exists already in the ground state for **HQC** and its methylated derivatives, is also formed in the excited state via intramolecular proton-transfer (ESIPT) processes. The proposed assignments of the multiple fluorescence bands (Table S15, Supporting Information) are in qualitative agreement with the results of ab initio CC2/cc-pVDZ computations (Table S13, Supporting Information). The calculations suggest that the trace of emissions of **H4MQC** and **H2MQC** at about ∼21600 and ∼22600 cm^{-1}, respectively, correspond to the **IIa** rather than to the **IIb** form because the excited-state **IIb** form of **HQC** (Figure 11) and **H4MQC**,[53] contrary to **HMMQC** (Figure 12), would rather tend to dissipate its energy along the barrierless PT process toward the **NH**-excited state.

The absorption, fluorescence, and excitation spectra of **HMMQC** indicate that the excited-state long-range irreversible 7-quinolinol → 7(1*H*)-quinolinone (**OH** → **NH**) tautomerization is observed for this compound. The ^{1}H NMR investigations and electronic absorption spectra prove that the **OH** form is dominant in the ground state. On the other hand, the spectral position and shape of the single emission band of **HMMQC** suggests that the luminescence corresponds to only one excited-state species, analogous to that which is responsible in **HQC** for the long-wave emission (i.e., the **NH** form). The corresponding Stokes shift is as large as 8000 cm^{-1} in *n*-hexane and about 9200 cm^{-1} in polar and protic solvents with respect to the lowest absorption band assigned to the **OH** tautomer. There is no doubt that this fluorescence is related to the other form of the molecule, most probably to the **NH** tautomer. It is confirmed by the finding that the position and shape of **HMMQC** fluorescence in acetonitrile and in alcohols (centered at ∼19400 cm^{-1}) are very similar to those in water at pH = 7 observed at 19600 cm^{-1} upon direct excitation of the **NH** tautomer (Figure 3 in part 2[81]). Thus, although in the ground state either we do not observe the **NH** form (in low-polarity media) or its fraction is negligibly small (in acetonitrile and in alcohols), this tautomer is created via excited-state proton-transfer (ESPT) processes and is responsible for the observed emission. This conclusion is in agreement with the finding that the excitation spectra monitored in various parts of the fluorescence spectra match well the corresponding absorption spectra. There is little doubt, however, that the emission in nonpolar medium (*n*-hexane) can correspond to two forms (**IIb** and **III**). The ab initio CC2 computations (Figure 12 and Table S13, Supporting Information) predict that in vacuum the energies of fluorescence transitions $S_0 \leftarrow {}^1(\pi,\pi^*)$ for these forms are nearly identical and are in very good agreement with the experimental value of 21000 cm^{-1} (Table 5). Moreover, the minimum-energy profile of the $^1(\pi,\pi^*)$ excited state connecting these two forms indicates a low barrier (0.23 eV, 5.3 kcal mol^{-1}) that separates these two excited-state minima. The hypothesis of two emissions can be definitively excluded by the analysis of the solvent effects on the fluorescence quantum yields and decay times of **HMMQC** (see below); the results indicate that the fluorescence in various

dx.doi.org/10.1021/jp403621p | J. Phys. Chem. A 2013, 117, 9127−9146

Table 5. Solvent Effects on the Spectral Positions of Room-Temperature Fluorescence Maxima ($\tilde{\nu}_{fl}$, cm^{-1}), Quantum Yields (Φ_f) Determined for Various Excitations (λ_{exc}, nm), Lifetimes (τ, ns) and Resulting (Eqs S1−S3, Supporting Information) Nonradiative (k_{nr}, 10^8 s^{-1}) and Radiative (k_f, 10^7 s^{-1}) Rate Constants, and Electronic Transition Dipole Moments Corresponding to Fluorescence (M_{fl}, D) of 7-HQCs

compound	solvent	λ_{exc} [b]	Φ_f [a]	$\tilde{\nu}_{fl}$ [c]	τ [a]	k_{nr}	k_f	M_{fl}
HQC	HEX	345	0.005	19500/20500				
				ca. 24400				
	EA	345	0.006	20100				
				ca. 24000				
	ACN	356	0.01	20200				
		380	0.04	20200				
	1-PrOH	345	0.018	20700				
	MeOH	343	0.035	20700				
H2MQC	HEX	346	0.002	19900/20900	<0.4			
				ca. 22600				
				ca. 24000				
	EA	346	0.005	20900	<0.4			
				ca. 23000				
	ACN	346	0.01	20600				
		380	0.045	20600	0.9	10.6	5.0	2.7
	1-PrOH	346	0.02	20900				
		380	0.064	20900	0.9	10.4	7.1	3.1
	MeOH	346	0.045	20600				
HPQC	HEX	350	0.003	18100/19200	4.0			
				ca. 20500				
				ca. 24000	2.2			
	EA	350	0.005	ca. 20000	5.7[d] and ~0.8			
				21500	<0.5[d] and 4.4			
				23300				
	ACN	350	0.013	19600	4.0			
				21500				
				ca. 23500	<0.05[d] and 2.7			
	1-PrOH	350	0.022	19500	3.9[d] and <0.3			
				22600				
	MeOH	350		19100				
HMMQC	HEX	346	0.039	21000	1.5	6.4	2.6	1.9
	EA	346	0.037	20300	1.4	6.9	2.6	2.0
	ACN	346	0.035	19700	1.6	6.0	2.2	1.9
	1-PrOH	346	0.04	19700	1.8	5.3	2.2	1.9
	MeOH	346	0.023	19400				

[a]Estimated error: 10%. Thus, the maximum error is about 20% for the rate constants k_{nr} and k_f and about 10% for the transition moment M_{fl}. [b]Scatter of results: ±2.0 nm. [c]Scatter of results: ±150 cm^{-1}. [d]Dominant contribution.

solvents corresponds to only one and the same excited-state species (the experiments in water prove that it is the **NH** form).

It is noticeable that the calculations (Table S13, Supporting Information) suggest that the lowest excited singlet states are of the (n,π^*) nature. To gain more insight into the electronic structure of the emitting electronic states, solvent effects on the fluorescence quantum yield (Φ_f) and decay times (τ) of **H2MQC**, **HMMQC**, and **HPQC** were examined. These data and the resulting (see eqs S1−S4, Supporting Information)[106,107] radiative k_f and nonradiative k_{nr} rate constants, as well as the electronic transition dipole moments M_{fl} and M_{abs} of the fluorescence and related to the lowest $^1(\pi,\pi^*) \leftarrow S_0$ absorption transition, respectively, for the representatives of **7-HQCs** are collected in Table 5 (all the obtained data are presented in Table S15, Supporting Information).

The decay of the **HMMQC** fluorescence in a nanosecond (and picosecond[108]) range is single exponential; the values of Φ_f of 3−4% and $\tau \cong 1.6$ ns (τ values do not depend on the monitored emission wavelengths) are similar for the whole range of solvents. Fluorescence transition dipole moments $M_f \cong 1.9$ (±0.2) D of **HMMQC** (being the best quantitative measure of the transition probability) are slightly smaller than those estimated for the absorption of the **OH** tautomeric form ($M_{abs} \cong 2.5$ D); both values are independent of the solvent. These values, as well as the radiative rate constants $k_f \approx 2.4 \times 10^7$ s^{-1} prove the allowed character of the absorption and luminescence transitions. Without any doubt: (i) the observed absorption and emission spectra correspond to the excited $^1(\pi,\pi^*)$ states, and (ii) the only one and the same excited-state species is responsible for the emission in the nonpolar, polar aprotic, and protic media.

The fluorescence quantum yields of **HQC**, **H2MQC**, and **H4MQC** were measured upon excitation into two absorption bands (Table 5; Table S15, Supporting Information) corresponding (i) mainly to the **OH** tautomer (~28900 cm^{-1}) and (ii) to the **NH** tautomer (~26300 cm^{-1}). The direct excitation of the **NH** tautomer of **H2MQC** results in the quantum yield values about 3−5 times higher than those

dx.doi.org/10.1021/jp403621p | J. Phys. Chem. A 2013, 117, 9127−9146

obtained upon higher energy excitation. This interesting result seems to support a strong nonradiative decay of the transient intermediates **IIa** and **IIb**, which was theoretically predicted in the excited-state route of a formation of the **NH** form (Scheme 1,[50−53] Figures 11 and 12). Fluorescence lifetimes in the nanosecond range were measured monitoring different parts of the emission spectrum. The decay times for **H2MQC** in low-polarity media are too short to be measured correctly, in acetonitrile and in 1-propanol the lifetimes of the fluorescent state are about 0.9 ns. The resulting values of the radiative rate constants $k_f \approx (5-7) \times 10^7$ s^{-1} and of the fluorescence transition dipole moments $M_f \approx 2.7-3.1$ D prove the $^1(\pi,\pi^*)$ nature of the fluorescent state.

The room-temperature absorption spectra of **HPQC** (Figure 2) and **HMPQC** (Figure 5) in acetonitrile and in alcohols,

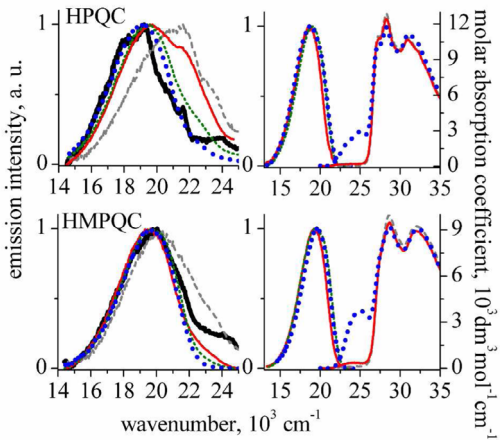

Figure 5. Room-temperature absorption and corrected and normalized fluorescence spectra (full thick lines (black), *n*-hexane; dashed thin lines (gray), ethyl acetate; full thin lines (red), acetonitrile; dotted thin lines (green), 1-propanol; dotted thick lines (blue), methanol) of **HPQC** and **HMPQC**. Left: fluorescence spectra upon excitation at 28170 cm^{-1}. Right: absorption and fluorescence spectra in acetonitrile and methanol upon excitation at 25000 cm^{-1}. Concentrations of the compounds were in the range from 10^{-5} to 10^{-4} mol dm^{-3}.

similarly to **HQC** and its methylated derivatives, show the low-energy absorption bands centered at about 400−420 nm, which indicates the formation of the **NH** tautomer already in the ground state. The shape and spectral position of the fluorescence spectra of **HPQC** and **HMPQC** (Figure 5), contrary to the other **7-HQCs** under study, depend on excitation. The direct excitation of the **NH** tautomeric form of **HPQC** in polar media at 410 nm (~24400 cm^{-1}) results in a single emission band centered at 18700 cm^{-1} (in acetonitrile), 18800 cm^{-1} (in methanol), and 19100 cm^{-1} (in 1-propanol). The spectral position of this fluorescence is similar to that recorded for the other compounds under study. It is noticeable that in highly protic methanol solutions, even upon high-energy excitation, only low-energy emission assigned to the **NH** tautomer is observed. On the other hand, two (or even three) emissions of **HPQC** are observed upon excitation at 325 nm (~30770 cm^{-1}, not shown) and 355 nm (~28170 cm^{-1}) in nonpolar and polar aprotic solvents as well as in 1-propanol. The dominant band in acetonitrile, which is centered at 19700 cm^{-1}, originates from the **NH** tautomer. The shoulder recorded at ca. 21400 cm^{-1} is probably due to the emission from the form **IIa** or **IIb** (Figure 1), being a transient product of the ESIPT reaction, and the long blue tail (a distinct emission band centered at ~24000 cm^{-1} is observed upon excitation at 325 nm) seems to correspond to the **OH** form (similarly to the Varma's interpretation[54,105] of the triple emission of **7HMMQ**, Figure 1). The fluorescence excitation spectra of **HPQC** in acetonitrile are in agreement with this assignment (Figure 6).

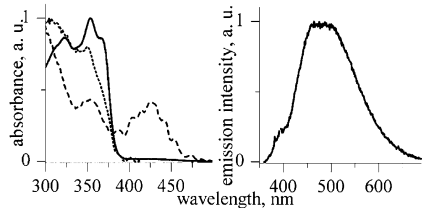

Figure 6. Right panel: room-temperature emission of **HPQC** in acetonitrile. Left panel: absorption (full line) and fluorescence excitation spectra monitored at the short-wave, i.e., between 425 and 465 nm (dotted line), and at the long-wave (between 500 and 555 nm, dashed line) parts of the emission band. See text for details.

The fluorescence monitored between 18000 and 20000 cm^{-1} is preferentially excited at the long-wave absorption band. On the other hand, the emission monitored at about 21500−23500 cm^{-1} is excited from the high-energy absorption bands. Similar effects are observed for **HMPQC**. The direct excitation of the **NH** tautomer at 24400 cm^{-1} leads to a single emission band centered at 19300 cm^{-1} (in acetonitrile), 19600 cm^{-1} (in 1-propanol) and 19700 cm^{-1} (in methanol). The shape of the fluorescence spectra recorded upon excitation at 28570 cm^{-1} suggests the presence of two emissions, which most probably correspond to the **OH** (the shoulder at ~23600 cm^{-1}) and the **NH** (the dominant band centered at about 19600 cm^{-1}) tautomeric forms.

The fluorescence spectrum of **HPQC** in *n*-hexane, in addition to the low-energy fluorescence from the **NH** form, shows a clear high-energy emission band of low intensity at about 24000 cm^{-1}, which can be attributed to the **OH** tautomer. The spectral position and shape of the fluorescence spectrum in ethyl acetate indicate three emissions. Most probably, the **OH** and **NH** tautomers are responsible for the shoulders observed at about 23500 and 20000 cm^{-1}, respectively. The maximum of the emission spectrum centered at ~21500 cm^{-1} is assigned to the intermediate product **IIa** or **IIb** of the ESIPT reaction (Scheme 2). This finding, which is similar to the luminescence properties of **7HMMQ**,[54,105] manifests that the **NH** tautomer, which in part exists in the ground state, is formed also in the excited state via an ESIPT reaction.

The results of time-resolved fluorescence investigations in the nanosecond range (Table 5) are in agreement with this interpretation. Fluorescence decays in ethyl acetate can be satisfactorily fitted to a sum of two exponentials. Varying the detection wavenumber from ~19500 to ~21700 cm^{-1} decreases the contribution of the long component and increases that of the short-lived component. The decay in acetonitrile also shows the long and short (too short to be determined with subnanosecond resolution) components. Measurements in *n*-hexane exhibit different results: the decay of the long-wave and the short-wave parts of the fluorescence spectrum is monoexponential, but the lifetimes are different, 4 and 2.2 ns, respectively.

dx.doi.org/10.1021/jp403621p | J. Phys. Chem. A 2013, 117, 9127−9146

Low-Temperature Investigations of 7-HQCs. The temperature effects on the absorption spectra of **H4MQC** in 1-propanol (Figure 7) show an increase of intensity of the long-wave absorption band with the decrease of temperature. Similar effects are observed in acetonitrile. The stabilization of the **NH** tautomeric form with lowering of temperature is most probably due to the increase of the solvent polarity; the dielectric constants of 1-propanol[109] and acetonitrile[110] increase with lowering of temperature. Interesting spectral changes are observed for the higher energy bands: the spectral positions of both bands shift to higher energy; for example, the maximum of the band centered at 28900 cm^{-1} at room temperature shifts to 30030 cm^{-1} at 133 K, and the band observed at 32570 cm^{-1} at 298 K disappears at 133 K. This finding indicates that, in agreement with theoretical ab initio and TD-DFT computations (Table 2 and Table S3, Supporting Information), the electronic transitions related to the various tautomeric forms of the molecule lie close to each other in this spectral region. The temperature dependence of the NMR spectra of **H4MQC** in CD_2Cl_2, $CDCl_3$, CD_3CN, and CD_3OD, which do not show any signals from the **IIa** or **IIb** forms, proves that these bands originate from the **OH** and **NH** forms.

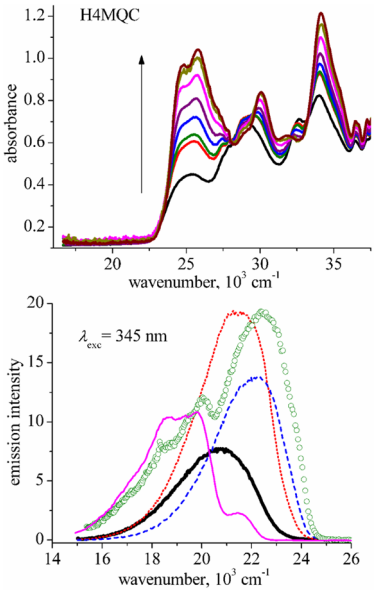

Figure 7. Temperature effects on the absorption (top panel, the spectra are recorded between 298 and 133 K; the arrow showing the decrease of temperature) and emission spectra upon excitation at ~29000 cm^{-1} (bottom panel) of **H4MQC** in 1-propanol. Bottom: room-temperature (full thick line, black) and low-temperature fluorescence spectra (dotted line, red, T = 173 K; dashed line, blue, T = 133 K) as well as total luminescence (open circles, green) and phosphorescence (full thin line, pink) in a glass at 77 K. The concentration of the solute is about 4 × 10^{-5} mol dm^{-3} at 293 K.

The lowering of temperature up to 173 K results in the increase of the intensity of the fluorescence spectra of **H4MQC** in 1-propanol solutions (Figure 7); further lowering of temperature leads to the shift of the fluorescence maximum from 20800 cm^{-1} at room temperature to 22200 cm^{-1} in a strongly viscous solution at 133 K. Notably, the total luminescence spectrum in rigid glass at 77 K shows two distinct bands centered at 22500 and 20000 cm^{-1}, and a shoulder at about 18500 cm^{-1}. The latter two transitions correspond to phosphorescence.

The temperature dependence of the fluorescence of **HPQC** in 1-propanol solutions (Figure 8) recorded upon direct excitation of the **NH** form shows similar effects to those observed for **H4MQC**. The fluorescence maximum shifts from 19100 cm^{-1} at room temperature to ~20900 cm^{-1} in a strongly viscous solution at 133 K and to about 21300 cm^{-1} at 77 K. This spectral shift can hardly be explained by the fluorescence of any other form than the **NH** tautomer. On the other hand, the temperature effects on the fluorescence of **HPQC** in 1-propanol observed upon excitation at 355 nm are in agreement with a hypothesis of the multiple fluorescence. In addition to the shift of the fluorescence maximum from ~19500 cm^{-1} at room temperature to ~21200 cm^{-1} in a strongly viscous solution at 133 K, the low-temperature spectrum shows two shoulders at ~23200 and ~25300 cm^{-1}. The latter spectral features can be assigned to the **OH** tautomeric forms of **HPQC** and **HPQ** (as an impurity, see next section), respectively.

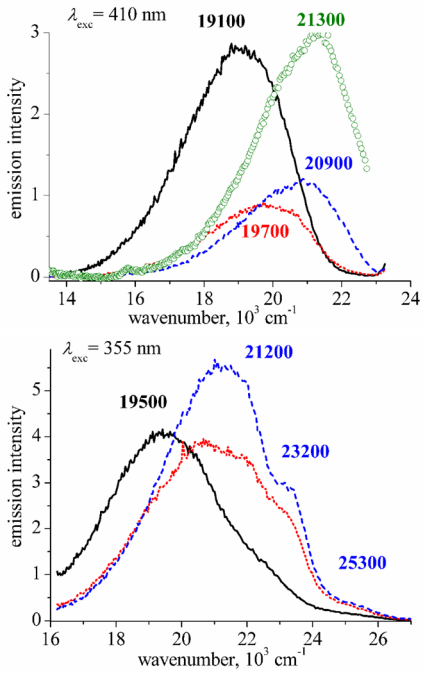

Figure 8. Room-temperature (full lines, black) and low-temperature fluorescence spectra (dotted lines, red, T = 173 K; dashed lines, blue, T = 133 K) and total luminescence spectra at 77 K (open circles, green) of **HPQC** in 1-propanol for various excitations. Top: direct excitation of the **NH** tautomeric form at 24400 cm^{-1}. Bottom: excitation of the **OH** and **NH** forms at 28170 cm^{-1}. The concentration of the solute is about 4 × 10^{-5} mol dm^{-3} at 293 K.

Photophysics of 7-Hydroxyquinolines (7-HQs). The analysis of the fluorescence spectra of the studied **7-HQCs** is performed under the assumption that the observed spectral features do not correspond to those of (i) the corresponding **7-HQs** (Scheme 4), the synthetic precursors of the former compounds and (ii) to the photoproducts (see below). To confirm the postulated origin of the emission bands discussed above, the spectra of the representatives of **7-HQCs** are compared with those of the corresponding **7-HQs** in Figure 9 (all the obtained absorption and fluorescence data in nonpolar and polar aprotic solvents, as well as in alcohols, are collected in Table 1 and in Table S16, Supporting Information, respectively).

dx.doi.org/10.1021/jp403621p | J. Phys. Chem. A 2013, 117, 9127−9146

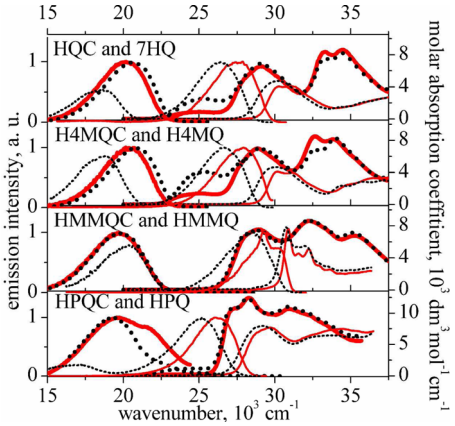

Figure 9. Comparison of the room-temperature absorption and corrected and normalized fluorescence spectra (full lines, red, acetonitrile; dotted lines, black, 1-propanol) of the representatives of **7-HQCs** (thick lines) and corresponding **7-HQs** (thin lines). Concentrations of the compounds are in the range from 10^{-5} to 10^{-4} mol dm^{-3}.

The spectral locations of the absorption and fluorescence bands of **7-HQs** are similar to those previously observed for 7-hydroxyquinoline (**7-HQ**),[55,67] **H2MQ** and **HDMQ**.[111] Therefore, it is natural to assign these bands to the same tautomeric species. The lack of the absorption band at about 25000 cm^{-1} for all the studied **7-HQs** (except **HDMQ** in methanol, Table 1) proves that the compounds exist in the ground state as the **OH** form (7-quinolinol). The **7-HQs** show, upon excitation, a single fluorescence band, assigned to the **OH** tautomer, at about 28000 cm^{-1} (**7-HQ** and its methyl derivatives), ~30000 cm^{-1} (**HMMQ**), and ~26500 cm^{-1} (**HPQ**, **HMPQ**) in nonpolar and polar aprotic media and dual luminescence phenomenon in alcohols (the short-wave and long-wave bands correspond to the **OH** and 7(1*H*)-quinolinone (**NH**) forms, respectively).[62−67,69] Both bands are markedly blue-shifted (the short-wave band) or red-shifted (the long-wave band, except **HMMQ**) with respect to the fluorescence spectra observed for the **7-HQCs**.

Experiments in Mixed Solvents. In **7-HQ** the acidic hydroxyl group and the basic nitrogen atom in the ring are too far apart to form an intramolecular hydrogen bond. Thus, the phototautomerization of **7-HQ** is observed only in protic solvents (e.g., alcohols). The long-wave band of **7-HQ** in alcohols was previously attributed to the **NH** form created by the excited-state triple proton transfer in the cyclic hydrogen-bonded complexes of 1:2 stoichiometry.[63−67,69] These bands for all the **7-HQs** except for **HMMQ** are markedly red-shifted with respect to the fluorescence of **7-HQCs**. The excited-state reorganization of the geometry of the majority of complexes to make it suitable for the ESPT process (Scheme 3) and the resulting ground-state destabilization energies can be the reason for this significant red shift.[67,69] On the contrary, the long-wave fluorescence band of **HMMQ** is slightly shifted to the blue with respect to the fluorescence of **HMMQC**. Most probably, the tautomerization of **HMMQ** is restricted to a particular complex of a cyclic geometry that is formed already in the ground state. To gain more insight into the ground-state formation of the complexes between **7-HQs** and an alcohol partner, titration experiments of **HMMQ** and **HPQ** in *n*-hexane solution with 1-butanol were performed (the solubility of the other **7-HQs** in *n*-hexane is too low to measure the changes in the absorption and fluorescence spectra). The spectrophotometric titration of **HMMQ** solutions (Figure 10), at alcohol concentrations low

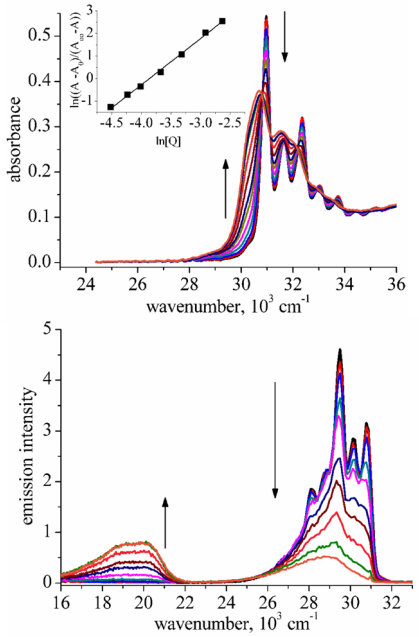

Figure 10. Titration of **HMMQ** solution in *n*-hexane with 1-butanol at 293 K. Top: changes in absorption. Bottom: evolution of both fluorescence bands. The arrows show spectral changes accompanying the addition of alcohol. The alcohol concentration varied from 0.0018 to 0.18 mol dm^{-3}. The inset in the absorption part shows the determination of the stoichiometry of the complex (eqs 1 and 2) from the absorption data recorded at 30300 cm^{-1}; A_0 and A_∞ denote the optical density measured when only the bare or complexed forms are present, and A is the optical density measured at an alcohol concentration [Q].

enough to prevent the formation of alcohol oligomers,[30,31] results in an appearance of isosbestic points in absorption (which indicates an equilibrium between two ground-state species: most probably uncomplexed **HMMQ** and the alcohol complex) and leads to the determination of the 1:2 stoichiometry of the complexes. For a reaction involving one chromophore molecule X and n alcohol molecules Y:[30]

$$X + nY = XY_n \tag{1}$$

the equilibrium constant, K_{1n}, may be expressed as

$$K_{1n} = \frac{[XY_n]}{[X][Y]^n} \qquad K_{1n} = \frac{A - A_0}{(A_\infty - A)[Q]^n} \tag{2}$$

where A_0 and A_∞ denote the absorbance measured when only the bare or complexed forms are present, respectively, and A is the absorbance measured at an alcohol concentration [Q]. From the plot of $\ln[(A - A_0)/(A_\infty - A)]$ vs $\ln[Q]$ one may obtain n, the number of alcohol molecules in the complex.

The appearance of 1:2 hydrogen-bonded complexes of **HMMQ** is followed by dual luminescence: the decrease of the intensity of the short-wave fluorescence (assigned to the **OH** tautomer) is accompanied by the appearance and growth of the low-energy band attributed to the **NH** (7(1*H*)-quinolinone) form. This finding supports our interpretation: **HMMQ** shows the ground-state formation of the 1:2 complex prepared for the excited-state proton-transfer process. Contrary to that, the titration of **HPQ** does not lead to unequivocal results, as the

dx.doi.org/10.1021/jp403621p | J. Phys. Chem. A 2013, 117, 9127−9146

absorption spectra do not show distinct isosbestic points. This suggests that, even at low alcohol concentration, various hydrogen-bonded **HPQ** complexes of different structure and stoichiometry are formed.

It should be noted that the titration experiments for **H4MQC**, **H2MQC**, **HPQC**, and **HMMQC** in *n*-hexane solution with 1-butanol and 1-propanol, contrary to the case of **7-HQs**, do not show any significant changes in the absorption spectra. In an attempt to gain more insight into the ground-state formation of the complexes between **7-HQCs** and an protic partner preliminary ab initio computations were performed for the **HQC** complexes with water of the 1:2 stoichiometry as the simplest and most probable representatives of the hydrogen-bonded clusters (see below).

Photostability. Finally, it should be stressed that the studied **7-HQCs**, except **HMMQC**, are not photostable. The UV irradiation of these compounds at 254 nm leads to photoproducts which emit short-wave fluorescence in the region of ~355−375 nm (about 26650−28200 cm^{-1}). One of the possible photoreactions, similarly to the case of benzaldehyde,[112,113] is a decomposition of a particular **7-HQC** compound into a respective **7-HQ** molecule and carbon monoxide (the Norrish type I reaction).[114] The preliminary NMR investigations of **HPQC** in CD_3CN, however, do not show any trace of **HPQ** upon intensive irradiation at 254 nm. On the other hand, the disappearance of the electronic absorption and fluorescence bands of **HPQC** in acetonitrile under the same irradiation conditions is followed by the appearance of the bands characteristic for **HPQ**. To understand the mechanism of the photoreactions, further studies have to be performed.

Theoretical Analysis. To get more insight into the photophysics of **7-HQCs**, the potential-energy profiles of the ground state (MP2 method) and the lowest excited singlet states (CC2 method) were computed for **HQC** and **HMMQC** under vacuum conditions along the minimum-energy path that connects the **OH** and **NH** tautomeric forms (Figures 11 and 12, respectively). The challenging question is a difference in photophysical properties between **HMMQC** and other **7-HQCs**.

It was previously theoretically predicted[51] that the energy landscape of both excited states, $^1(n,\pi^*)$ and $^1(\pi,\pi^*)$, is dependent on the position of substitution and the π-electron-donating ability of the substituent group to the **7-HQ** frame. The substitution of **7-HQ** in the 2-, 4-, or 6-positions by dimethylamino and/or amino groups, contrary to the methylation in any position, was predicted to decrease the energies of the $^1(\pi,\pi^*)$ states with respect to those of the $^1(n,\pi^*)$ states and the excited-state barrier from the **III** form toward the **IIb** form. These observations were in line with previous experimental studies on the effects of alkyl substituents on the ESIPT process in alkyl derivatives of 2,5-bis(2-benzoxazolyl)phenol.[115]

The shape of the energy profiles of **HQC** (Figure 11) in the ground state and in the lowest excited $^1(n,\pi^*)$ and $^1(\pi,\pi^*)$ states is indeed almost the same as for **H4MQC**.[53] Thus, **HQC** can be treated as a good representative of the whole group of its methyl substituted derivatives, as well as of **HPQC**.[116] The energy landscapes of **HQC** and **HMMQC** (Figure 12), ranging from the Franck−Condon region of the **OH** tautomer (form **I**, left-side of panel a) to the conical intersection (**CI**) region (panel b) look very similar. It is predicted for both compounds that (i) the optical excitation to the lowest $^1(\pi,\pi^*)$ state induces

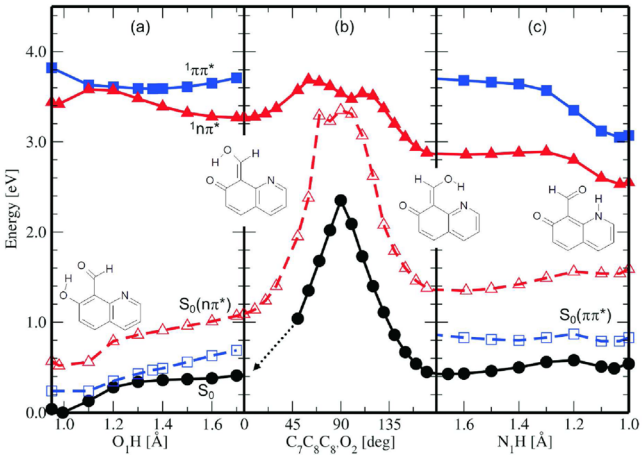

Figure 11. Energy profiles of **HQC** in the ground-state S_0 (circles) and in the lowest excited states, $^1(n,\pi^*)$ (triangles) and $^1(\pi,\pi^*)$ (squares), computed at the MP2/cc-pVDZ and CC2/cc-pVDZ levels, respectively, along the minimum-energy path (solid) for hydrogen transfer from the **OH(I)** tautomer to the **IIa** form (O_1H distance, a), for protonated carbaldehyde−ring torsion (b), and for hydrogen transfer **IIb** ↔ **III(NH)** (N_1H distance, c). $S_0(n,\pi^*)$ and $S_0(\pi\pi^*)$ (dashed curves) denote the "vertical"-energy profile of the ground state, computed along the minimum-energy path of the respective, $^1(n,\pi^*)$ or $^1(\pi,\pi^*)$, excited state. The structures of the **I**, **IIa**, **IIb**, and **III** forms correspond to the ground state (see text and Scheme 2).

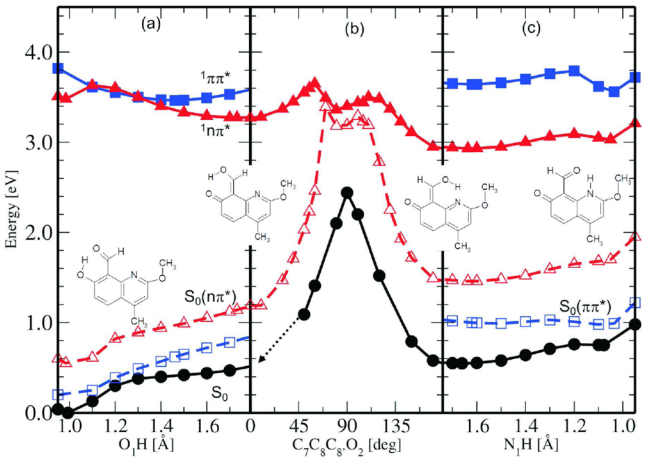

Figure 12. Energy profiles of **HMMQC** in the ground-state S_0 (circles) and in the lowest excited states, $^1(n,\pi^*)$ (triangles) and $^1(\pi,\pi^*)$ (squares), computed at the MP2/cc-pVDZ and CC2/cc-pVDZ levels, respectively, along the minimum-energy path (solid) for hydrogen transfer from the **OH(I)** tautomer to the **IIa** form (O_1H distance, a), for protonated carbaldehyde−ring torsion (b), and for hydrogen transfer **IIb** ↔ **III(NH)** (N_1H distance, c). $S_0(n,\pi^*)$ and $S_0(\pi\pi^*)$ (dashed curves) denote the "vertical"-energy profile of the ground state, computed along the minimum-energy path of the respective, $^1(n,\pi^*)$ or $^1(\pi,\pi^*)$, excited state. The structures of the **I**, **IIa**, **IIb**, and **III** forms correspond to the ground state (see text and Scheme 2).

along the O_1H bond a barierrless ESIPT process from the **OH** tautomer to the **IIa** form, which is more exoenergetic for **HMMQC** due to the π-electron-donating character of the methoxy group; (ii) the **IIa** form is highly unstable in the ground-state S_0. The twisting motion around the $C_8-C_{8'}$ bond (**IIa** ↔ **IIb** process) abruptly raises the energy of the ground and the lowest excited $^1(n,\pi^*)$ states and drives the systems

dx.doi.org/10.1021/jp403621p | J. Phys. Chem. A 2013, 117, 9127−9146

(albeit with a barrier) toward the **CI** region for a twist angle between 60° and 120°. The observed efficient radiationless depopulation of the fluorescent states of **7-HQCs** (Table 5) is in agreement with this prediction. The CC2 optimization with broken C_s symmetry of the energy profile of the higher-excited $^1(\pi,\pi^*)$ state was not possible, due to its collapse to a lower-lying $^1(n,\pi^*)$ state.

The exoenergetic, barrierless ESIPT process from the **IIb** form to the **NH** tautomer (form **III**) for **HQC** is predicted for both lowest excited states (panel c). Thus, the traces of fluorescence experimentally observed at about 22000 cm^{-1} for **H2MQC** and **H4MQC** (Figure 4, Table S15, Supporting Information) seem to correspond to the **IIa** form rather than to the **IIb** form. On the contrary, the energies of these forms of **HMMQC** in the $^1(n,\pi^*)$ or $^1(\pi,\pi^*)$ states are very similar and a barrier to the ESIPT reaction **IIb** ↔ **III** is expected to be of 0.23 eV (5.3 kcal/mol). Moreover, the calculated fluorescence transitions $S_0 \leftarrow {}^1(\pi,\pi^*)$ for the **IIb** form (~21200 cm^{-1}) and the **NH** tautomer (~20700 cm^{-1}, Table S13, Supporting Information) are in a very good agreement with the experimental value of 21000 cm^{-1} in *n*-hexane (Table 5). Therefore, theoretical calculations do not allow us to distinguish unambiguously which form is responsible for the observed emission of **HMMQC**. The **HMMQC** fluorescence is assigned to the **NH** form due to the findings: (i) that the position and shape of fluorescence in acetonitrile and in alcohols are very similar to those in water at pH = 7 obtained upon direct excitation of the **NH** tautomer (part 2)[81] and (ii) the only one and the same excited-state species is responsible for the emission in the nonpolar, polar aprotic, and protic media (Table 5).

The MP2-computed relative energies of the **IIb** and **NH** forms of **HQC** in the ground-state S_0 are very similar (panel c); the **NH** tautomer is predicted to be more stabilized than the **IIb** form by about 0.5 kcal mol^{-1} (~0.02 eV, Tables S1–S4, Supporting Information). Contrary to that, the **NH** form of **HMMQC** is predicted to be higher in energy by about 2.8 kcal mol^{-1} (~0.12 eV, Table S5, Supporting Information) than the **IIb** form. These results, however, are not in agreement with NMR investigations, which indicate that the forms **IIb** of the studied **7-HQCs** are not present in the ground state (Table 4).

Finally, in an attempt to gain more insight into the ground-state formation of the complexes between **7-HQCs** and an alcohol partner, the preliminary ab initio computations were performed for the **HQC** complexes with water of the 1:2 stoichiometry (Figure 13). The two geometries: **I.w2** (corresponding to the 1:2 complex of the form **OH** of **HQC**) and **III.w2** (complex of the **NH** form), were optimized in the ground state with the aug-cc-pVDZ basis set to properly reproduce intermolecular hydrogen bonds in the so-called "discrete model" of a solvent. Even though the water dimer in the two starting geometries was arranged to make a "double-water" bridge to allow for the proton transfer for either the form **I.w2** (**OH**) or **III.w2** (**NH**), the resulting optimized geometry did not resemble the proton-bridge-like structure anymore. For example, for the form **III.w2** (**NH**) the closest water (first hydrate shell) makes a bond with the 7 oxygen atom, whereas the other water molecule makes a hydrogen bond with the first-shell water only, being far away from the "reaction center". For the **I.w2** form the closest water (first-hydrate shell) makes a hydrogen bond with the azine nitrogen atom, nonprotonated in this form, whereas the second-hydrate-shell water molecule makes a hydrogen bond with the first water but does not make a second hydrogen bond with the 7-hydroxyl group. This implies that the intramolecular bonds are probably stronger than the intermolecular bonds that form 7HQ···H_2O and H_2O···H_2O complexes. This conclusion may support the crane mechanism against the solvent-assisted one; however, more water molecules are needed to support this statement.

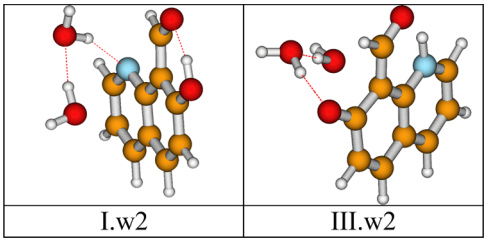

Figure 13. Ground-state equilibrium geometries of the HQC···$(H_2O)_2$ clusters corresponding to the forms **OH** (**I.w2**) and **NH** (**III.w2**) optimized at the MP2/aug-cc-pVDZ level.

Moreover, the relative energy $\Delta H = E(\mathrm{III}) - E(\mathrm{I})$ of 5.3 kcal mol^{-1} is lower in the discrete model than the corresponding ΔH value for the isolated **HQC** molecule, 9.7 kcal mol^{-1} (Table 6), according to the results obtained at the MP2/augg-cc-pVDZ level.

Table 6. Simulation of the Effect of Water on the Relative Energies (kcal mol^{-1}) of the Tautomeric Forms of HQC (Explanation in Text)[a]

		HQC	
form/environment	method	I	III
HQC in vacuum	MP2	0.00	9.7
HQC in water	MP2+PCM	0.00	6.5
HQC···$(H_2O)_2$ in vacuum	MP2	0.00	5.3
HQC···$(H_2O)_2$ in water	MP2+PCM	0.00	1.8

[a]The results were obtained within the PCM model at the MP2/aug-cc-pVDZ level of theory.

Instead of adding more water molecules into the system, an additional effort was made to link the two models: the discrete and the polarizable-continuum model (PCM). The PCM single-point calculations, with water as a solvent, were performed on top of the MP2-optimized geometries of the HQC···$(H_2O)_2$ cluster. These results gave additional stabilization of the complex **III.w2** (**NH**) (Table 6) in comparison to the discrete model. These results predict that the water should stabilize the more polar (**III**) form. Additionally, they support the crane mechanism vs the solvent-assisted one because the intramolecular hydrogen bonds linking the frame and the crane units seem to be stronger and dominate over the intermolecular hydrogen bonds linking **HQC** with the molecules of solvent.

4. SUMMARY AND CONCLUSIONS

The comparative studies of the spectroscopy and photophysics of the series of 7-hydroxyquinoline-8-carbaldehydes (**7-HQCs**) and 7-hydroxyquinolines (**7-HQs**) allow us to understand the solvent-dependent mechanism of the ground- and excited-state long-range prototropic tautomerization.

The electronic absorption spectra (Figure 9; Table S16, Supporting Information) indicate that the 7-quinolinol (**OH**)

dx.doi.org/10.1021/jp403621p | J. Phys. Chem. A 2013, 117, 9127–9146

forms of all the studied 7-hydroquinolines (**7-HQs**), similarly to **7-HQ**, are dominant in the ground state in aprotic solvents and in alcohols. The compounds show a single short-wave fluorescence band in aprotic solvents and two emission bands in alcohols. The short-wave and long-wave bands correspond to the **OH** and 7(1*H*)-quinolinone (**NH**) tautomers (its resonance hybrid is a zwitterionic species **Z**), respectively. The latter is most probably created by the excited-state triple proton transfer in the hydrogen-bonded complexes of 1:2 stoichiometry. Interestingly, **HMMQ**, contrary to the other compounds, shows the ground-state formation of this complex which is prepared for the ESIPT process.

Contrary to the case of studied **7-HQs**, the NMR and electronic absorption investigations prove the presence of the **OH** and **NH** tautomers already in the ground state for all the studied **7-HQCs**, except for **HMMQC**. The fraction of the **NH** form increases with the increase of polarity and hydrogen bond donor ability of the surrounding environment. The change in the relative populations of these forms with changes of temperature provides evidence for thermal equilibrium. Therefore, there must be a possibility of conversions **I** → **III** and **III** → **I** in solution in the electronic ground state. The NMR spectra of **7-HQCs** show two sets of proton signals even at room temperature; i.e., they are in the regime of slow exchange. The mechanism of this conversion most probably involves the interactions with the solvent molecules. The comparison of the dependence of the electronic absorption spectra on solvent properties with the results of NMR investigations allows us to assign the long-wave band at about 25000 cm^{-1} to the **NH** tautomer. **HMMQC** does not show this band (except for aqueous solutions, see part 2[81]) and exists in the ground state nearly exclusively as the **OH** tautomer. These experimental findings are qualitatively corroborated by the theoretical computations predicting that (i) the **OH** form should be dominant in the ground state for all the studied molecules, (ii) the ground-state destabilization energy of the **NH** tautomer with respect to the **OH** form of **HMMQC** is considerably higher than that of the other **7-HQCs**, and (iii) the **NH** form should be stabilized in polar and protic media.

For all the studied **7-HQCs** except **HPQC**, the dominant fluorescence in aprotic media and in alcohols can be attributed to the $^1(\pi,\pi^*)$ excited state of the **NH** tautomer. This is confirmed by direct excitation of this tautomer (see also the comparison with the emission of the protonated cations and deprotonated anions in part 2[81]). The multiple, solvent- and excitation-dependent, fluorescence of **HPQC** most probably originates from (i) the **OH** tautomer (~23300−23600 cm^{-1}), (ii) the intermediate transient product **IIa** or **IIb** (Scheme 2) of the excited-state intramolecular proton transfer, ESIPT (~21500 cm^{-1}), and (iii) the **NH** tautomer (~19200−19700 cm^{-1}), which in part originates from the ground state and in part is formed in the excited state via ESIPT processes. The fluorescence of **HQC** and its methyl derivatives, **H2MQC**, **H4MQC**, and **HDMQC**, in nonpolar and low-polarity media show two emission bands assigned to the **OH** tautomer (~24000−24500 cm^{-1}) and to the **NH** tautomer (~20500−21000 cm^{-1}). The single emission band of **HMMQC**, observed at about 19400−21000 cm^{-1} is attributed to the **NH** tautomer, which is formed via ESIPT process. The multiple or single fluorescence behavior of **7-HQCs** can be correlated with electron-withdrawing/donating properties of a substituent (of which the strongest donor is the methoxy group). **HPQC** shows fluorescence of the substrate (the **OH** tautomer), transient (probably the **IIa** form) and product (the **NH** form) of the excited-state tautomerization. The ESIPT process is most efficient in **HMMQC**, as only the emission of the **NH** tautomer is observed for this compound. Different luminescent properties of **HMMQC** with respect to **HQC** (and the other **7-HQCs**) are probably due to the smaller height of the energy barrier along the excited-state path corresponding to carbaldehyde−hydroxyquinoline ring torsion (**IIa** → **IIb**) in the former and the resulting faster kinetics with respect to the latter. This hypothesis, however, is not confirmed by computations. **HMMQC** seems to be a good model to study dynamics and kinetics of the excited-state tautomerization process due to the fact that the **OH** tautomer (which is the substrate of the photoreaction) is a major form of the compound in the ground state.

The mechanism of the excited-state tautomerization of **7-HQCs** is surely different from that of the ground state and of much faster kinetics. The tautomerization process in aprotic media seems to be intramolecular, as it is observed in nonpolar solvents. At least two different mechanisms can be discussed: the "transmitter" and "crane" models. The first one, similarly to 3-hydroxypyridine-2-carboxylic acid,[117,118] involves a transfer of two protons O═C—H and O—H, the former being transferred to the ring nitrogen atom. This process cannot be definitively excluded, although it seems to be less probable. The NMR experiments clearly show that, in both the ground and excited states, the exchange of the CHO aldehyde proton with deuterons from the protic solvent (CD_3OD) can be excluded, as the CHO group does not undergo deuteration. More probably, the mechanism seems to involve two irreversible adiabatic proton-transfer processes connected with a twist of the proton crane, as proposed by Varma and co-workers.[54] The electronic excitation of the **OH** form induces proton transfer along the hydrogen bond, resulting in the structure **IIa** (Scheme 1).[50−53] The next step, which involves twisting around a single covalent bond connecting the 7-hydroxyquinoline moiety with the carbaldehyde group, leads to the form **IIb**. The second PT process results in the tautomeric form **NH**. However, the time-resolved nano- and picosecond[108] fluorescence investigations of **HMMQC** in such strongly viscous medium as paraffin do not show any measurable rise of the **NH** fluorescence. Most probably, the excited-state process is too short to be measured with the resolution of about 10−15 ps. The very efficient radiationless depopulation of the fluorescent states of **7-HQCs** is in agreement with the theoretical ab initio computations predicting the conical intersection on the route of the ESIPT process under vacuum conditions.[50−53]

In alcohol and water (see part 2[81]) solutions, however, the mechanism of PT reactions in **7-HQCs** seems to involve additional reactions producing various hemiacetals or hydrates, respectively, which are in dynamic equilibria with the **OH** and **NH** tautomers (Scheme 5). In such excited supermolecules the water or alcohol molecules may act as proton-relay systems, which can efficiently transform the **OH** tautomer into the **NH** tautomer. The driving force for the ESIPT reaction is the increase of acidity of the hydroxyl group and the increase of basicity of the quinoline nitrogen atom upon electronic excitation. The results of our investigations of the prototropic reactions in acidic and basic acetonitrile and water solutions of **7-HQCs** (part 2)[104] indicate, similarly to **7-HQs**,[60,108] a shift toward the **NH** form upon excitation and prove the opposite pK_a tendencies of the acidic and basic centers of the compounds.

dx.doi.org/10.1021/jp403621p | J. Phys. Chem. A 2013, 117, 9127−9146

Scheme 5. Hypothetical Dynamic Equilibria between 7-Quinolinol (OH, Left) and 7(1*H*)-Quinolinone (NH, Right) Tautomers of HQC and Respective Hydrates in Aqueous Solutions

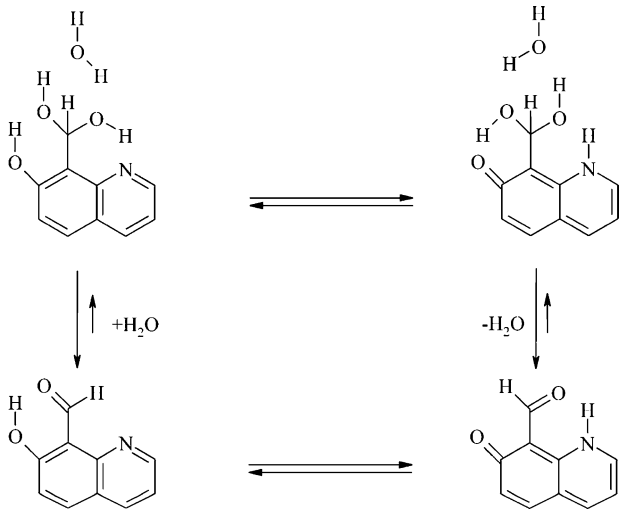

■ ASSOCIATED CONTENT

Supporting Information

Synthesis and identification of 7-hydroxyquinolines and 7-hydroxyquinoline-8-carbaldehydes. Radiative rate constants and electronic transition dipole moments. Computations of 7-hydroxyquinolines and 7-hydroxyquinoline-8-carbaldehydes, including neutral forms of **7HQC** derivatives, vertical excitation energies, excitation wavelength, oscillator strengths, dipole moments, adiabatic energies, and solvent effects on relative energies and spectral positions. This material is available free of charge via the Internet at http://pubs.acs.org.

■ AUTHOR INFORMATION

Corresponding Author

*J. Herbich: e-mail, herbich@ichf.edu.pl; fax, + 48 (22) 3433333.

Notes

The authors declare no competing financial interest.

■ ACKNOWLEDGMENTS

This work was supported by grants NN 204 264 238 and NN 204 239 134 from the Ministry of Science and Higher Education, and grants 2011/01/M/ST2/00561 and 3550/B/H03/2011/40 from the Polish National Science Centre. The technical assistance of Mrs. Anna Zielińska is greatly appreciated.

■ REFERENCES

(1) Bell, R. P. *The Proton Transfer in Chemistry*; Chapman & Hall: London, 1973.

(2) Bell, R. P. *The Tunnel Effect in Chemistry*; Chapman & Hall: London, 1980.

(3) Arnaut, L. G.; Formosinho, S. J. Excited-State Proton Transfer Reactions I. Fundamentals and Intermolecular Reactions. *J. Photochem. Photobiol. A: Chem.* **1993**, *75*, 1−20.

(4) Ormson, S. M.; Brown, R. G. Excited state Intramolecular Proton Transfer. Part 1. ESIPT to Nitrogen. *Prog. React. Kinet.* **1994**, *19*, 45−91.

(5) Le Gourrierec, D.; Ormson, S. M.; Brown, R. G. Excited State Intramolecular Proton Transfer. Part 2. ESIPT to Oxygen. *Prog. React. Kinet.* **1994**, *19*, 211−275.

(6) Catalán, J.; del Valle, J. C.; Kasha, M. Resolution of Concerted Versus Sequential Mechanisms in Photo-Induced Double-Proton Transfer Reaction in 7-Azaindole H-Bonded Dimer. *Proc. Natl. Acad. Sci. U. S. A.* **1999**, *96*, 8338−8343.

(7) Waluk, J. Conformational Aspects of Intra- and Intermolecular Excited State Proton Transfer. In *Conformational Analysis of Molecules in Excited States*; Waluk, J., Ed.; Methods in Stereochemical Analysis Series; Wiley-VCH: Weinheim, 2000; Chapter 2, pp 57−111; see also references therein.

(8) Waluk, J. Hydrogen-Bonding-Induced Phenomena in Bifunctional Heteroazaaromatics. *Acc. Chem. Res.* **2003**, *36*, 832−838.

(9) Waluk, J. Ground- and Excited-State Tautomerism in Porphycenes. *Acc. Chem. Res.* **2006**, *39*, 945−952.

(10) Sekiya, H.; Sakota, K. Excited-State Double-Proton Transfer in a Model DNA Base Pair: Resolution for Stepwise and Concerted Mechanism Controversy in the 7-Azaindole Dimer Revealed by Frequency- and Time-Resolved Spectroscopy. *J. Photochem. Photobiol. C: Photochem. Rev.* **2008**, *9*, 81−91.

(11) Mühlpfordt, A.; Even, U.; Ernsting, N. P. Zero-Kinetic-Energy Photoelectron Spectroscopy and Excited-State Intramolecular Proton Transfer in a 'Double' Benzoxazole. *Chem. Phys. Lett.* **1996**, *263*, 178−184.

(12) Heimbrook, L. A.; Kenny, J. E.; Kohler, B. F.; Scott, B. W. Dual Fluorescence Excitation Spectra of Methyl Salicylate in a Free Jet. *J. Chem. Phys.* **1981**, *75*, 5201−5203.

(13) Heimbrook, L. A.; Kenny, J. E.; Kohler, B. F.; Scott, B. W. Lowest Excited Singlet State of Hydrogen-Bonded Methyl Salicylate. *J. Phys. Chem.* **1983**, *87*, 280−289.

(14) Felker, P. M.; Lambert, W. R.; Zewail, A. H. Picosecond Excitation of Jet-Cooled Hydrogen-Bonded Systems: Dispersed Fluorescence and Time-Resolved Studies of Methyl Salicylate. *J. Chem. Phys.* **1982**, *77*, 1603−1606.

(15) Herek, J. L.; Pedersen, S.; Bañares, S.; Zewail, A. H. Femtosecond Real-Time Probing of Reactions. IX. Hydrogen-Atom Transfer. *J. Chem. Phys.* **1992**, *97*, 9046−9062.

(16) Douhal, A.; Lahmani, F.; Zewail, A. H. Proton-Transfer Reaction Dynamics. *Chem. Phys.* **1996**, *207*, 477−498.

(17) Bisht, P. B.; Petek, H.; Yoshihara, K.; Nagashima, U. Excited-State Enol-Keto Tautomerization in Salicylic Acid: A Supersonic Free Jet Study. *J. Chem. Phys.* **1995**, *103*, 5290−5308.

(18) Lahmani, F.; Zehnacker-Rentien, A. Effect of Substitution on the Photoinduced Intramolecular Proton Transfer in Salicylic Acid. *J. Phys. Chem.* **1997**, *101*, 6141−6147.

(19) Nishiya, T.; Yamauchi, S.; Hirota, N.; Baba, M.; Hanazaki, L. Fluorescence Studies of Intramolecularly Hydrogen-Bonded o-Hydroxyacetophenone, Salicylamide, and Related Molecules. *J. Phys. Chem.* **1986**, *90*, 5730−5735.

(20) Su, C.; Lin, J. Y.; Hsieh, R. M. R.; Cheng, P. Y. Coherent Vibrational Motion During the Excited-State Intramolecular Proton Transfer Reaction in o-Hydroxyacetophenone. *J. Phys. Chem. A* **2002**, *1061*, 11997−12001.

(21) Kijak, M.; Nosenko, Y.; Singh, A.; Thummel, R. P.; Waluk, J. Mode-Selective Excited-State Proton Transfer in 2-(2′-Pyridyl)pyrrole Isolated in a Supersonic Jet. *J. Am. Chem. Soc.* **2007**, *129*, 2738−2739.

(22) Morgan, P. J.; Fleisher, A. J.; Vaquero-Vara, V.; Pratt, D. W.; Thummel, R. P.; Kijak, M.; Waluk, J. Excited-State Proton Transfer in *syn*-2-(2′-Pyridyl)pyrrole Occurs on the Nanosecond Time Scale in the Gas Phase. *J. Phys. Chem. Lett.* **2011**, *2*, 2114−2117.

(23) Taylor, C. A.; El-Bayoumi, M. A.; Kasha, M. Excited-State Two-Proton Tautomerism in Hydrogen-Bonded N-Heterocyclic Base Pairs. *Proc. Natl. Acad. Sci. U. S. A.* **1969**, *63*, 253−260.

(24) Ingham, K. C.; Abu-Elgheit, M.; El-Bayoumi, M. A. Confirmation of Biprotonic Phototautomerism in 7-Azaindole Hydrogen-Bonded Dimers. *J. Am. Chem. Soc.* **1971**, *93*, 5023−5025.

(25) Ingham, K. C.; El-Bayoumi, M. A. Photoinduced Double Proton Transfer in a Model Hydrogen Bonded Base Pair. Effects of

Temperature and Deuterium Substitution. *J. Am. Chem. Soc.* **1974**, *96*, 1674−1682.
(26) Avouris, P.; Yang, L. L.; El-Bayoumi, M. A. Excited State Interactions of 7-Azaindole with Alcohol and Water. *Photochem. Photobiol.* **1976**, *24*, 211−216.
(27) Chang, C.; Shabestary, N.; El-Bayoumi, M. A. Excited-State Double Proton Transfer in 1-Azacarbazole Hydrogen-Bonded Dimers. *Chem. Phys. Lett.* **1980**, *75*, 107−109.
(28) Waluk, J.; Komorowski, S. J.; Herbich, J. Excited-State Double Proton Transfer in 1-Azacarbazole-Alcohol Complexes. *J. Phys. Chem.* **1986**, *90*, 3868−3871.
(29) Waluk, J.; Herbich, J.; Oelkrug, D.; Uhl, S. Excited-State Double Proton Transfer in the Solid State: The Dimers of 1-Azacarbazole. *J. Phys. Chem.* **1986**, *90*, 3866−3868.
(30) Herbich, J.; Hung, C.-Y.; Thummel, R. P.; Waluk, J. Solvent-Controlled Excited State Behavior: 2-(2′-Pyridyl)indoles in Alcohols. *J. Am. Chem. Soc.* **1996**, *118*, 3508−3518.
(31) Kyrychenko, A.; Herbich, J.; Wu, F.; Thummel, R. P.; Waluk, J. Solvent-Induced *syn*−*anti* Rotamerization of 2-(2′-Pyridyl)indole and the Structure of its Alcohol Complexes. *J. Am. Chem. Soc.* **2000**, *122*, 2818−2827.
(32) Nosenko, Y.; Wiosna-Sałyga, G.; Kunitski, M.; Petkowa, I.; Singh, A.; Buma, W. J.; Thummel, R. P.; Brutschy, B.; Waluk, J. Proton transfer with a twist? Femtosecond Dynamics of 7-(2-Pyridyl)indole in Condensed Phase and in Supersonic Jets. *Angew. Chem.-Int. Ed.* **2008**, *47*, 6037−6040.
(33) Wiosna-Sałyga, G.; Nosenko, Y.; Kijak, M.; Thummel, R. P.; Brutschy, B.; Waluk, J. Structure and Hydrogen-Bond Vibrations of Water Complexes of Azaaromatic Compounds: 7-(3′-Pyridyl)indole. *J. Phys. Chem. A* **2010**, *114*, 3270−3279.
(34) Herbich, J.; Dobkowski, J.; Thummel, R. P.; Hedge, V.; Waluk, J. Intermolecular Excited State Double Proton Transfer in Dipyridocarbazole: Alcohol Complexes. *J. Phys. Chem.* **1997**, *101*, 5839−5845.
(35) Marks, D.; Zhang, H.; Borowicz, P.; Waluk, J.; Glasbeek, M. Subpicosecond Fluorescence Upconversion Studies of Intermolecular Proton Transfer of Dipyrido[2,3-a:3′,2′-i]carbazole and Related Compounds. *J. Phys. Chem. A* **2000**, *104*, 7167−7175.
(36) Kijak, M.; Zielińska, A.; Thummel, R. P.; Herbich, J.; Waluk, J. Photoinduced Double Proton Transfer in Water Complexes of 1H-Pyrrolo[3,2-H]quinoline and Dipyrido[2,3-a:3′,2′-i]carbazole. *Chem. Phys. Lett.* **2002**, *366*, 329−335.
(37) del Valle, J. C.; Dominguez, E.; Kasha, M. Competition between Dipolar Relaxation and Double Proton Transfer in the Electronic Spectroscopy of Pyrroloquinolines. *J. Phys. Chem. A* **1999**, *103*, 2467−2475.
(38) Kyrychenko, A.; Herbich, J.; Izydorzak, M.; Wu, F.; Thummel, R. P.; Waluk, J. Role of Ground State Structure in Photoinduced Tautomerization in Bifunctional Proton Donor−Acceptor Molecules: 1H-Pyrrolo[3,2-h]quinoline and Related Compounds. *J. Am. Chem. Soc.* **1999**, *121*, 11179−11188.
(39) Nosenko, Y.; Kunitski, M.; Thummel, R. P.; Kyrychenko, A.; Herbich, J.; Waluk, J.; Riehn, C.; Brutschy, B. Detection and Structural Characterization of Clusters with Ultrashort-Lived Electronically Excited States: IR Absorption Detected by Femtosecond Multiphoton Ionization. *J. Am. Chem. Soc.* **2006**, *128*, 10000−10001.
(40) Nosenko, Y.; Kyrychenko, A.; Thummel, R. P.; Waluk, J.; Brutschy, B.; Herbich, J. Fluorescence Quenching in Cyclic Hydrogen-Bonded Complexes of 1H-Pyrrolo[3,2-h]quinoline with Methanol: Cluster Size Effect. *Phys. Chem. Chem. Phys.* **2007**, *9*, 3276−3285.
(41) Nosenko, Y.; Kunitski, M.; Riehn, C.; Thummel, R. P.; Kyrychenko, A.; Herbich, J.; Waluk, J.; Brutschy, B. Separation of Different Hydrogen-Bonded Clusters by Femtosecond UV-Ionization-Detected Infrared Spectroscopy: 1H-Pyrrolo[3,2-h]quinoline·$(H_2O)_n$=1,2 Complexes. *J. Phys. Chem. A* **2008**, *112*, 1150−1156.
(42) Kijak, M.; Zielińska, A.; Chamchoumis, C.; Herbich, J.; Thummel, R. P.; Waluk, J. Conformational Equilibria and Photo-induced tautomerization in 2-(2′-Pyridyl)pyrrole. *Chem. Phys. Lett.* **2004**, *400*, 279−285.
(43) Rode, M. F.; Sobolewski, A. L. Photophysics of Inter- and Intra-Molecularly Hydrogen-Bonded Systems: Computational Studies on the Pyrrole−Pyridine Complex and 2(2′-Pyridyl)pyrrole. *Chem. Phys.* **2008**, *347*, 413−421.
(44) Kasha, M.; Horowitz, P.; El-Bayoumi, M. A. *Molecular Spectroscopy: Modern Research*; Academic Press: New York, 1972; p 287.
(45) Goodman, M. F. Mutations Caught in the Act. *Nature* **1995**, *378*, 237−238.
(46) Douhal, A.; Kim, S. K.; Zewail, A. H. Femtosecond Molecular Dynamics of Tautomerization in Model Base Pairs. *Nature* **1995**, *378*, 260−263.
(47) Folmer, D. E.; Poth, L.; Wisniewski, E. S.; Castleman, A. W., Jr. Arresting Intermediate States in a Chemical Reaction on a Femtosecond Time Scale: Proton Transfer in Model Base Pairs. *Chem. Phys. Lett.* **1998**, *287*, 1−7.
(48) Catalán, J.; del Valle, J. C.; Kasha, M. Conformity of the 7-Azaindole Dimer Cationic Potential with Photoionization/Coulomb-Explosion MS Observations and the Concerted Biprotonic Transfer Mechanism. *Chem. Phys. Lett.* **2000**, *318*, 629−636.
(49) Folmer, D. E.; Wisniewski, E. S.; Castleman, A. W., Jr. Excited State Double Proton Transfer in the 7-Azaindole Dimer Revisited. *Chem. Phys. Lett.* **2000**, *318*, 637−643.
(50) Sobolewski, A. L. Reversible Molecular Switch Driven by Excited-State Hydrogen Transfer. *Phys. Chem. Chem. Phys.* **2008**, *10*, 1243−1247.
(51) Rode, M. F.; Sobolewski, A. L. Effect of Chemical Substituents on the Energetical Landscape of a Molecular Photoswitch: an Ab Initio Study. *J. Phys. Chem. A* **2010**, *114*, 11879−11889.
(52) Benesch, C.; Rode, M. F.; Čížek, M.; Härtle, R.; Rubio-Pons, O.; Thoss, M.; Sobolewski, A. L. Switching the Conductance of a Single Molecule by Photoinduced Hydrogen Transfer. *J. Phys. Chem. C* **2009**, *113*, 10315−10318.
(53) Lapinski, L.; Nowak, M. J.; Nowacki, J.; Rode, M. F.; Sobolewski, A. L. A Bistable Molecular Switch Driven by Photo-induced Hydrogen-Atom Transfer. *ChemPhysChem* **2009**, *10*, 2290−2295.
(54) Jalink, C. J.; van Ingen, W. M.; Huizer, A. H.; Varma, C. A. G. O. Prospects for Using Photoinduced Intramolecular Proton Transfer to Study the Dynamics of Conformational Changes in Flexible Molecular Chains. *J. Chem. Soc., Faraday Trans.* **1991**, *87*, 1103−1109.
(55) Ewing, G. W.; Steck, E. A. Absorption Spectra of Heterocyclic Compounds. I. Quinolinols and Isoquinolinols. *J. Am. Chem. Soc.* **1946**, *68*, 2181−2187.
(56) Albert, A.; Phillips, J. N. Ionization Constants of Heterocyclic Substances. Part II. Hydroxy-Derivatives of Nitrogenous Six-Membered Ring-Compounds. *Chem. Soc.* **1956**, 1294−1304.
(57) Mason, S. F. The Tautomerism of N-heteroaromatic Hydroxy-Compounds. Part I. Infrared Spectra. *Chem. Soc.* **1957**, 4874−4880.
(58) Mason, S. F. The Tautomerism of N-heteroaromatic Hydroxy-Compounds. Part II. Ultraviolet Spectra. *Chem. Soc.* **1957**, 5010−5017.
(59) Mason, S. F. The Tautomerism of N-heteroaromatic Hydroxy-Compounds. Part III. Ionisation Constants. *Chem. Soc* **1958**, 674−685.
(60) Mason, S. F.; Philp, J.; Smith, B. E. Prototropic Equilibria of Electronically Excited Molecules. Part II. 3-, 6-, and 7-Hydroxyquinoline. *J. Chem. Soc. A.* **1968**, 3051−3056.
(61) Schulman, S.; Fernando, Q. Excited State Prototropic Equilibria of Some Quinolinols. *Tetrahedron* **1968**, *24*, 1777−1783.
(62) Thistlewaite, P. J.; Corkill, P. J. Direct Observation of Phototautomerism Kinetics in 7-Quinolinol by Picosecond Spectroscopy. *Chem. Phys. Lett.* **1982**, *85*, 317−321.
(63) Thistlewaite, P. J. Solvation Effects in the Phototautomerization of 7-Quinolinol. *Chem. Phys. Lett.* **1983**, *96*, 509−512.
(64) Itoh, M.; Adachi, T.; Tokumura, K. Transient Absorption and Two-Step Laser Excitation Fluorescence Spectra of the Excited-State and Ground-State Proton Transfer in 7-Hydroxyquinoline. *J. Am. Chem. Soc.* **1983**, *105*, 4828−4829.

(65) Tokumura, K.; Itoh, M. Two-Photon-Induced Excited-State Proton Transfer Process in Methanol Solution of 7-Hydroxyquinoline. *J. Phys. Chem.* **1984**, *88*, 3921−3923.
(66) Itoh, M.; Adachi, T.; Tokumura, K. Time-Resolved Fluorescence and Absorption Spectra and Two-Step Laser Excitation Fluorescence of the Excited-State Proton Transfer in the Methanol Solution of 7-Hydroxyquinoline. *J. Am. Chem. Soc.* **1984**, *106*, 850−855.
(67) Konijnenberg, J.; Ekelmans, G. B.; Huizer, A. H.; Varma, C. A. G. O. Mechanism and Solvent Dependence of the Solvent-Catalysed Pseudo-Intramolecular Proton Transfer of 7-Hydroxyquinoline in the First Electronically Excited Singlet State and in the Ground State of its Tautomer. *J. Chem. Soc., Faraday Trans.* **1989**, *85*, 39−51.
(68) Lee, S. I.; Jang, D. J. Proton Transfers of Aqueous 7-Hydroxyquinoline in the First Excited Singlet, Lowest Triplet, and Ground States. *J. Phys. Chem.* **1995**, *99*, 7537−7541.
(69) Kohtani, S.; Tagami, A.; Nakagaki, R. Excited-state Proton Transfer of 7-Hydroxyquinoline in a Non-Polar Medium: Mechanism of Triple Proton Transfer in the Hydrogen-Bonded System. *Chem. Phys. Lett.* **2000**, *316*, 88−93.
(70) Lahmani, F.; Douhal, A.; Breheret, E.; Zehnacker-Rentien, A. Solvation Effects in Jet-Cooled 7-Hydroxyquinoline. *Chem. Phys. Lett.* **1994**, *220*, 235−242.
(71) Bach, A.; Leutwyler, S. Water-Chain Clusters: Vibronic Spectra of 7-Hydroxyquinoline·$(H_2O)_n$, n=1−4. *Chem. Phys. Lett.* **1999**, *299*, 381−388.
(72) Fang, W. H. Ab Initio Study of the Triple-Proton-Transfer Reactions of Ground and Excited States of 7-Hydroxyquinoline in Methanol Solution. *J. Am. Chem. Soc.* **1998**, *120*, 7568−7576.
(73) Fang, W. H. Theoretical Characterization of the Structures and Reactivity of 7-Hydroxyquinoline−$(H_2O)_n$ (n = 1−3) Complexes. *J. Phys. Chem. A* **1999**, *103*, 5567−5573.
(74) Kim, T. G.; Kim, Y.; Jang, D. J. Catalytic Roles of Water Protropic Species in the Tautomerization of Excited 6-Hydroxyquinoline: Migration of Hydrated Proton Clusters. *J. Phys. Chem. A* **2001**, *105*, 4328−4332.
(75) Poizat, O.; Bardez, E.; Buntix, G.; Alain, V. Picosecond Dynamics of the Photoexcited 6-Methoxyquinoline and 6-Hydroxyquinoline Molecules in Solution. *J. Phys. Chem. A* **2004**, *108*, 1873−1880.
(76) Yu, H.; Kwon, O. H.; Jang, D. J. Migration of Protons during the Excited-State Tautomerization of Aqueous 3-Hydroxyquinoline. *J. Phys. Chem. A* **2004**, *108*, 5932−5937.
(77) Park, H. J.; Kwon, O. H.; Ah, C. S.; Jang, D. J. Excited-State Tautomerization Dynamics of 7-Hydroxyquinoline in *β*-Cyclodextrin. *J. Phys. Chem. B* **2005**, *109*, 3938−3943.
(78) Kwon, O. H.; Kim, T. G.; Lee, Y. S.; Jang, D. J. Biphasic Tautomerization Dynamics of Excited 7-Hydroxyquinoline in Reverse Micelles. *J. Phys. Chem. B* **2006**, *110*, 11997−12004.
(79) Nagakawa, T.; Kohtani, S.; Itoh, M. Picosecond Fluorescence and Two-Step LIF Studies of the Excited-State Proton Transfer in Methanol Solutions of 7-Hydroxyquinoline and Methyl-Substituted 7-Hydroxyquinolines. *J. Am. Chem. Soc.* **1995**, *117*, 7952−7957.
(80) Kwon, O. H.; Doo, H.; Lee, Y. S.; Jang, D. J. Excited-State Proton-Relay Dynamics of 7-Hydroxyquinoline Embedded in a Solid Matrix of Poly(2-hydroxyethyl Methacrylate). *ChemPhysChem* **2003**, *4*, 1079−1083.
(81) Vetokhina, V.; Nowacki, J.; Pietrzak, M.; Rode, M. F.; Sobolewski, A. L.; Waluk, J.; Herbich, J. 7-Hydroxyquinoline-8-carbaldehydes. 2. Prototropic Equilibria. *J. Phys. Chem. A* **2013**, DOI: 10.1021/jp403623x.
(82) Cameron, M.; Hoerrner, R. S.; McNamara, J. M.; Figus, M.; Thomas, S. One-Pot Preparation of 7-Hydroxyquinoline. *Org. Process Res. Dev.* **2006**, *10*, 149−152.
(83) Fedoryak, O. D.; Dove, T. M. Brominated Hydroxyquinoline as a Photolabile Protecting Group with Sensitivity to Multiphoton Excitation. *Org. Lett.* **2002**, *4*, 3419−3422.
(84) Bülow, C.; Issler, G. Beitrag zur Kenntniss der Derivate des 7-Oxychinolins. *Chem. Ber.* **1903**, *36*, 4013−4019.
(85) Borsche, W. Über die Synthese *α*-substituierter Cinchoninsäuren nach Döbner. *Chem. Ber.* **1908**, *41*, 3884−3894.
(86) Kochańska, L.; Bobrański, B. Über den 7-Oxy-chinolin-aldehyd-(8). *Chem. Ber.* **1936**, *69B*, 1807−1813.
(87) Reichardt, C. *Solvent Effects in Organic Chemistry*; Ebel, H. F., Ed.; Monographs in Modern Chemistry, Vol. 3; Verlag Chemie: New York, Weinheim, 1979.
(88) Kamlet, M. J.; Abboud, J. L. M.; Taft, R. W. An Examination of Linear Solvation Energy Relationships. *Prog. Phys. Org. Chem.* **1981**, *13*, 485−630.
(89) Jasny, J. Multifunctional spectrofluorimetric system. *J. Lumin.* **1978**, *17*, 149−173.
(90) Velapoldi, R. A. Considerations on Organic Compounds in Solution and Inorganic Ions in Glasses as Fluorescent Standard Reference Materials. *Proc. Conf. NBS, National Bureau of Standards* **1972**, 231.
(91) Christiansen, O.; Koch, H.; Jørgensen, P. The Second-Order Approximate Coupled Cluster Singles and Doubles Model CC2. *Chem. Phys. Lett.* **1995**, *243*, 409−418.
(92) Hättig, C.; Weigend, F. CC2 Excitation Energy Calculations on Large Molecules Using the Resolution of the Identity Approximation. *J. Chem. Phys.* **2000**, *113*, 5154−5162.
(93) Hättig, C. Geometry Optimizations with the Coupled-Cluster Model CC2 Using the Resolution-of-the-Identity Approximation. *J. Chem. Phys.* **2003**, *118*, 7751−7762.
(94) Köhn, A.; Hättig, C. Analytic Gradients for Excited States in the Coupled-Cluster Model CC2 Employing the Resolution-of-the-Identity Approximation. *J. Chem. Phys.* **2003**, *119*, 5021−5037.
(95) Dunning, T. H. Gaussian Basis Sets for Use in Correlated Molecular Calculations. I. The Atoms Boron through Neon and Hydrogen. *J. Chem. Phys.* **1989**, *90*, 1007−1024.
(96) Miertus, S.; Scrocco, E.; Tomasi, J. Electrostatic Interaction of a Solute with a Continuum. A Direct Utilizaion of Ab Initio Molecular Potentials for the Prevision of Solvent Effects. *Chem. Phys.* **1981**, *55*, 117−129.
(97) Cammi, R.; Corni, S.; Mennucci, B.; Tomasi, J. Electronic Excitation Energies of Molecules in Solution: State Specific and Linear Response Methods for Nonequilibrium Continuum Solvation Models. *J. Chem. Phys.* **2005**, *122*, 104513−104525.
(98) Ahlrichs, R.; Bär, M.; Häser, M.; Horn, H.; Kölmel, C. Electronic structure Calculations on Workstation Computers: The Program System Turbomole. *Chem. Phys. Lett.* **1989**, *162*, 165−169.
(99) Weigend, F.; Häser, M.; Patzelt, H.; Ahlrichs, R. RI-MP2: Optimized Auxiliary Basis Sets and Demonstration of Efficiency. *Chem. Phys. Lett.* **1998**, *294*, 143−152.
(100) Frisch, M. J.; Trucks, G. W.; Schlegel, H. B.; Scuseria, G. E.; Robb, M. A.; Cheeseman, J. R.; Scalmani, G.; Barone, V.; Mennucci, B.; Petersson, G. A.; et al. *Gaussian 09*, Revision B.01; Gaussian, Inc.: Wallingford, CT, 2010.
(101) Frisch, M. J.; Trucks, G. W.; Schlegel, H. B.; Scuseria, G. E.; Robb, M. A.; Cheeseman, J. R.; Montgomery, J. A., Jr.; Vreven, T.; Kudin, K. N.; Burant, J. C.; et al. *Gaussian 03*, Revision B.03, Gaussian, Inc.: Pittsburgh, PA, 2003.
(102) Lee, C.; Yang, W.; Parr, R. G. Development of the Colle-Salvetti Correlation-Energy Formula into a Functional of the Electron Density. *Phys. Rev. B* **1988**, *37*, 785−789.
(103) Becke, A. D. Density-Functional Thermochemistry. III. The Role of Exact Exchange. *J. Chem. Phys.* **1993**, *98*, 5648−5652.
(104) Becke, A. D. Density-Functional Exchange-Energy Approximation with Correct Asymptotic Behavior. *Phys. Rev. A* **1988**, *38*, 3098−3100.
(105) Geerlings, J. D.; Huizer, A. H.; Varma, C. A. G. O. Long-Range Proton Transfer Catalysed by 1,4-Dioxane Proton Craning in a Non-Polar Medium. *J. Chem. Soc., Faraday Trans.* **1997**, *93*, 237−243.
(106) Birks, J. B. *Photophysics of Aromatic Molecules*; Wiley: New York, 1978.
(107) Michl, J.; Thulstrup, E. W. *Spectroscopy with Polarized Light*; Wiley: New York, 1986.
(108) Dobek, K. Private communication.

(109) Stickel, F.; Fischer, E. W.; Richert, R. Dynamics of Glass-Forming Liquids. II. Detailed Comparison of Dielectric Relaxation, DC-Conductivity, and Viscosity Data. *J. Chem. Phys.* **1996**, *104*, 2043−2056.
(110) Würflinger, A. Dielectric Measurements at High Pressures and Low-Temperatures. II. The Dielectric Constant at Acetonitrile. *Ber. Bunsen-Ges. Phys. Chem.* **1980**, *84*, 653−657.
(111) Senda, N.; Momotake, A.; Arai, T. Fluorescence Enhancement in 7-Hydroxyquinoline Analogs by Methyl Substitution and Their Spectroscopic Characteristics in Aqueous Solution. *Bull. Chem. Soc. Jpn.* **2010**, *83*, 1272−1274.
(112) Berger, M.; Goldblatt, I. L; Steel, C. Photochemistry of Benzaldehyde. *J. Am. Chem. Soc.* **1973**, *95*, 1717−1725.
(113) Feenstra, J. S.; Parks, S. T.; Zewail, A. H. Excited State Molecular Structures and Reactions Directly Determined by Ultrafast Electron Diffraction. *J. Chem. Phys.* **2005**, *123*, 221104−221110.
(114) Laue, Th.; Plagens, A. *Named Organic Reactions*, 2nd ed.; John Wiley & Sons: Chichester, England, New York, 2005; 320 pp, ISBN 0-40-01041-X.
(115) Luzina, E.; Sepiol, J.; Svartsov, N.; Grabowska, A. Effect of Alkyl Substituents on Excited State Intramolecular Proton Transfer Dynamics of Jet-Cooled bis(benzoxazolyl)phenoles. *J. Chem. Phys.* **2007**, *126*, 194308−194315.
(116) Oziminski, W. P.; Dobrowolski, J. Cz. σ- and π-Electron Contributions to the Substituent Effect: Natural Population Analysis. *J. Phys. Org. Chem.* **2009**, *22*, 769−778.
(117) Tang, K.-C.; Chen, C.-L.; Chuang, H.-H.; Chen, J.-L.; Chen, Y.-J.; Lin, Y.-C.; Shen, J.-Y.; Hu, W.-P.; Chou, P.-T. A Genuine Intramolecular Proton Relay System Undergoing Excited-State Double Proton Transfer Reaction. *J. Phys. Chem. Lett.* **2011**, *2*, 3063−3068.
(118) Rode, M. F.; Sobolewski, A. L. Ab Initio Study on the Excited-State Proton Transfer mediated Photophysics of 3-Hydroxy-Picolinic Acid. *Chem. Phys.* **2012**, *409*, 41−48.